

# Applications of Raman Spectroscopy in Pandemic Virology: A Comprehensive Review

Hulya Yilmaz, Anuradha Ramoji, Andreea Winterfeld, Hamideh Salehi, Aykut Ozkul, and Jürgen Popp\*

Cite This: <https://doi.org/10.1021/acsp Photonics.5c02174>

Read Online

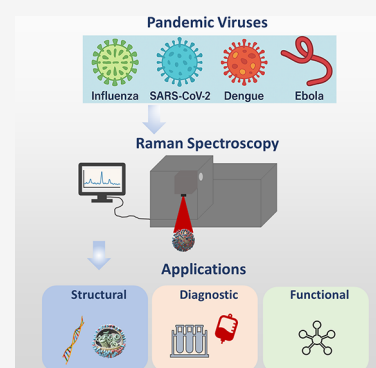
ACCESS |

Metrics & More

Article Recommendations

**ABSTRACT:** Raman spectroscopy, with its ability to provide molecular fingerprinting of biological samples, has recently emerged as a powerful technique in virology. Unfortunately, emerging and re-emerging viral pathogens with a rising threat highlight the urgent requirement for rapid, sensitive, and label-free diagnostic tools to monitor both viral presence and host responses. Recently, Raman spectroscopy use has increased not only in nonpandemic viruses but also in pandemic-prone viruses. This review presents a comprehensive analysis of Raman spectroscopy and its enhanced variants, such as surface-enhanced Raman spectroscopy (SERS), tip-enhanced Raman spectroscopy (TERS), and coherent Raman spectroscopies (CARS/SRS), in the context of pandemic virus research. By improving sensitivity, spatial resolution, and acquisition speed, these variants allow for quick and, in some cases, real-time analysis of viral particles and virus-host interactions in clinical samples and infected cells. A systematic evaluation of Raman-based methodologies was conducted across several virus families with pandemic potential, including Orthomyxoviridae, Coronaviridae, Filoviridae, Flaviviridae, and others, selected for their roles in past pandemics. Furthermore, prominent technical and virological obstacles hindering the expanded application of these methods were identified, alongside a discussion of prospective future directions for research and development. This effort aims to consolidate the current status of Raman spectroscopy in pandemic virology to enhance its integration into worldwide research on pandemic virus surveillance, pathogenesis, and diagnostics.

**KEYWORDS:** Raman spectroscopy, pandemic viruses, viral pathogenesis, virus-host interaction, biofluids analysis



## INTRODUCTION

The growing threat of highly pathogenic viruses continues to challenge global public health. Past and present outbreaks have shown how pandemic viruses strain health systems, economies, and societies.<sup>1</sup> These pathogens are often highly transmissible, mutate rapidly, and originate from animals, making continuous scientific progress and diagnostic innovation essential.<sup>2</sup> Traditional approaches such as microscopy, immunoassays, molecular biology, and proteomics have deepened our understanding of viral structure, replication, and host responses.<sup>3</sup> However, they often rely on labeling, are time-consuming, or require destructive processing, which limits their use in rapid, noninvasive diagnostics. Raman spectroscopy addresses many of these issues by providing label-free, molecular-level insights. It has advanced variants, including surface-enhanced Raman spectroscopy (SERS), tip-enhanced Raman spectroscopy (TERS), and coherent anti-Stokes Raman scattering (CARS), which offer high sensitivity and spatial resolution, enabling real-time monitoring of viruses and host–virus interactions in clinical samples.

To our knowledge, although several reviews broadly summarize Raman spectroscopy in virology, covering non-pandemic viruses and methods.<sup>2,24,30,31</sup> There is a lack of a pandemic-focused synthesis that connects Raman techniques to

high-risk virus families, biosafety concerns, and outbreak response needs. This review addresses that gap by categorizing Raman research based on virus families with pandemic potential and critically assessing their readiness for translation, factors behind their underrepresentation, and future preparedness strategies.

This review explores Raman spectroscopy with a focus on pandemic-prone viruses of global concern, including influenza, coronaviruses, filoviruses, and flaviviruses, and so on.<sup>1</sup> These families were chosen for their history of pandemics, zoonotic potential, transmissibility, and representation in Raman studies. The review first introduces these viruses and their transmission patterns, then compares conventional approaches to viral study. It goes on to discuss the principles, instrumentation, and applications of Raman spectroscopy, with examples highlighting spectral biomarkers, diagnostic performance, and methodologies. Finally, it examines current challenges, such as

**Received:** October 7, 2025

**Revised:** February 12, 2026

**Accepted:** February 17, 2026

**Table 1. Overview of Virus Classification According to Family, Type of Nucleic Acid in the Genome, Reservoir, and Transmission Modes along with Studies by Raman Spectroscopy Variants<sup>a</sup>,<sup>1,9–12</sup>**

viral family	type of nucleic acid in the genome	virus	reservoir	human infection from reservoir and human
Orthomyxoviridae	–ssRNA	Influenza virus	Wild waterfowl	– Airborne or close contact with infected animals
Filoviridae	–ssRNA	Marburg virus	Bats	– Contact/consumption of infected bats or intermediary hosts
		Ebola virus	Bats	– Direct contact with body fluids
Flaviviridae	–ssRNA	Dengue Virus	Arthropods	– Contact/consumption of infected bats or intermediary hosts
		Zika virus	Arthropods	– Direct contact with body fluids
Picornaviridae	+ssRNA	Echovirus	Anthroponotic	– Aedes species mosquitoes (Ae. aegypti or Ae. albopictus).
		Polio virus	Anthroponotic	– Arthropod-borne (mosquito bite) Perinatal, sexual contact
Poxviridae	dsDNA	Smallpox virus	Anthroponotic	– Fecal-oral transmission, respiratory droplets
		Monkeypox virus	Most likely small mammals	– N/A, -Fecal-oral transmission
Nairoviridae	–ssRNA	Crimean-Congo hemorrhagic fever	Arthropods (ticks)	– N/A, -Droplets (respiratory secretions)
Arenaviridae	–ssRNA	Lassa virus	Rodents (Mastomys species)	– Direct contact with infected animals
Coronaviridae	+nsRNA	SARS-CoV-2	Bats	– Close, personal contact; fomites; respiratory secretions
		MERS	Bats, camels	– Arthropod-borne
		SARS	Bats	– Direct contact with body fluids
Paramyxoviridae	–ssRNA	Nipah virus	Bats	– Contact with rodent urine or feces
Phenuiviridae	–ssRNA	Rift Valley fever virus	Arthropods (mosquitoes, ticks)	– Direct contact with body fluids
				– Consumption of infected bats or pigs, virus-contaminated fruits
				– Consumption of infected bats or pigs, virus-contaminated fruits-Respiratory secretions
				– Close contact with infected livestock
				– No human-to-human transmission

<sup>a</sup>MERS: Middle East respiratory syndrome, SARS: Severe acute respiratory syndrome, EVD: Ebola virus disease, DCDRS: Drop-coating deposition Raman spectroscopy, – ssRNA: Negative-stranded RNA, + ssRNA: Positive-stranded RNA, + nsRNA: nonsegmented positive-strand RNA, dsDNA: double-stranded DNA.

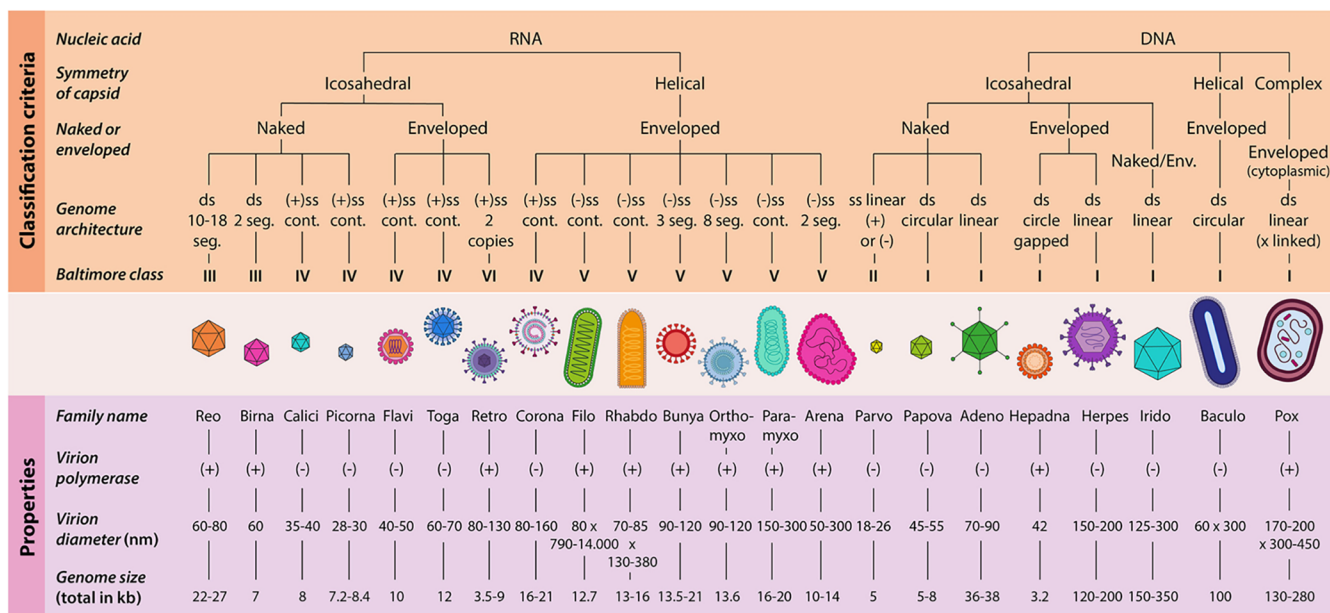


**Figure 1.** Overview of virion classification and their properties (Ramoji, A., Pahlow, S., Pistiki, A., Rueger, J., Shaik, T. A., Shen, H., Wichmann, C., Krafft, C., & Popp, J. (2022). *Understanding viruses and viral infections by biophotonic methods. Translational Biophotonics*, 4(1–2), e202100008. 10.1002/tbio.202100008). Reprinted from ref 2.

sensitivity limits, fluorescence interference, and biosafety requirements, and outlines future directions to advance Raman spectroscopy for pandemic preparedness and global health.

**Pandemic Viruses**

Recent historical progress in public health shows that viral diseases can quickly evolve into global disasters. An article comprehensively analyzes the factors contributing to pandemics

**Table 2. Overview of Technologies That Provide Information on Virus Visualization, Detection, and Interaction**

techniques	types	advantages	limitations	references
electron microscopy	microscopy	– High-resolution imaging of viral particles - No need for specific reagents tailored to identify the pathogenic organism.	– Requires extensive sample preparation and expensive equipment	3,13
confocal microscopy		– Visualization of virus localization in cells and tissue – Axial resolution in the range of 100–150 nm.	– Fluorescent labels requirement - Limited depth penetration - Potential for photobleaching - Requires extensive sample preparation and expensive equipment	
viral genome sequencing	molecular biology	– Precise identification of viral strains and mutations – Single-molecule long-read sequencing	– Requires high-quality nucleic acids and bioinformatics	15,14,21
reverse genetics		– Enables manipulation of viral genomes to study gene function	– Technically complex; requires a specialized system	
reporter assays		– Real-time monitoring of viral infection using reporter genes	– May require transgenic systems or cell line engineering	
gene knockdown/ knockout		– Targeted study of gene function in host-virus interactions	– Potential off-target effects; requires validation	
mass spectrometry	proteomics and metabolomics	– Sensitive detection of viral proteins and metabolites – Identifies direct and indirect molecular interactions	– High cost - Complex sample preparation and data analysis	6,16
enzyme-linked immunosorbent assay	immunological techniques	– Sensitive, high-throughput quantification of antigens or antibodies	– May produce false positives; requires careful controls	17,18
flow cytometry		– Rapid, multiparametric analysis of infected cells	– Requires labeled antibodies; limited to known targets	
immunohistochemistry		– Localizes viral antigens in tissue samples	– Relatively low throughput; dependent on antibody specificity	
viral entry assays	functional assays	– Quantifies viral entry efficiency into host cells	– Limited to in vitro systems; may not mimic in vivo conditions	7,19
viral replication assays		– Measures efficiency of viral genome replication	– May not distinguish between infectious and noninfectious particles	
cell viability assays		– Assesses cell health and cytopathic effects of viral infection	– May not directly measure viral activity	
computational modeling	systems biology	– Simulates infection dynamics; integrates large data sets	– Model assumptions require experimental validation	20

and underscores the importance of preparedness and research in controlling infectious diseases.<sup>1</sup> Pandemics such as the Spanish (influenza A/H1N1) flu (1918), Asian (influenza A/H2N2) flu (1957), Hong Kong (influenza A/H3N2) flu (1968), and re-emergence of A/H1N1 viruses (1977), as well as influenza A/H1N1 (2009), focusing on the specific subtypes of influenza A virus (IAV) involved, along with SARS-CoV-2 (2019), are discussed. It thoroughly analyzes the World Health Organization (WHO)'s approach to handling Public Health Emergencies of International Concern (PHEIC) and provides a comprehensive list of diseases with significant epidemic potential or inadequate countermeasures by addressing PHEIC and the WHO Priority Diseases Report. Additionally, a future pandemic could arise from zoonotic viruses transmitted by mammals or birds, highlighting airborne transmission as a key cause of human infection.<sup>1</sup> Table 1 provides a summary of pandemic virus families, animal reservoirs, and modes of transmission, offering an overview of pandemic viruses. To deepen the understanding of the pandemic potential of emerging viruses, it is crucial to examine not only epidemiological patterns but also the molecular and structural characteristics that allow viruses to infect, replicate, and spread effectively. These include the virus's genome type, mutation rate, host cell tropism, receptor-binding affinity, and mechanisms of immune evasion, all of which contribute to its adaptability and capacity for interspecies transmission.<sup>4–6</sup> RNA viruses, for instance, are particularly prone to high mutation rates, enabling rapid evolution and escape from host immune defenses. Structural elements such as envelope proteins play also a critical role in viral entry, host specificity, and transmissibility. Understanding these

viral characteristics is essential for predicting which pathogens may present the greatest threat and for designing targeted antiviral interventions.<sup>6</sup> Figure 1 provides a visual summary of virion classification based on structural and genomic features, including nucleic acid type, capsid symmetry, envelope presence, genome architecture, and Baltimore classification.<sup>2</sup> This framework contextualizes viral diversity and public health relevance and provides a foundation for understanding virus-host interactions. These interactions are dynamic processes that govern viral life cycles, pathogenesis, and host immune responses, and are therefore central to therapeutic development.<sup>6,7</sup> A range of complementary techniques is used to investigate virus-host interactions, each offering distinct mechanistic<sup>8</sup> insights, as discussed in the following sections.

### Conventional Techniques for Virus Structure, Function, and Host Interaction

Understanding of viral pathogenesis and host responses requires multidisciplinary tools probing structural, molecular, and functional aspects of infection. Traditional methods are presented with a comparative overview of the leading technologies used for imaging, molecular detection, and interaction studies in Table 2. Briefly, Microscopy techniques, including electron and confocal microscopy,<sup>13</sup> provide high-resolution visualization of viral particles, entry, replication, and assembly within host cells, but require extensive preparation, fluorescence labeling, and high costs.<sup>3,8</sup> Molecular biology techniques, including genome sequencing, reverse genetics, gene knockdown/knockout, and reporter assays, enable dissection of viral gene function, replication dynamics, and

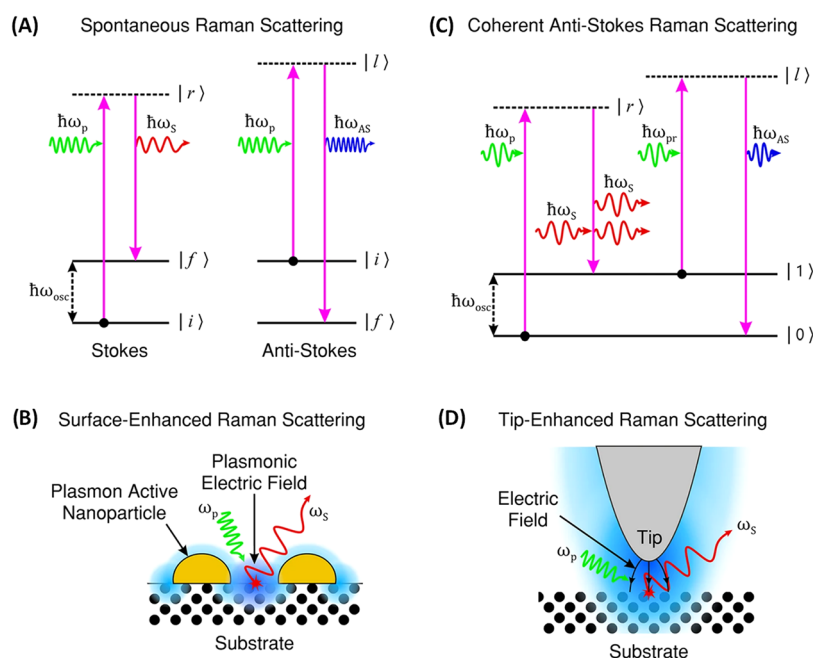


**Figure 2.** (A) Illustration of Stokes and anti-Stokes Raman scattering, showing energy transitions during spontaneous inelastic light scattering. (Anti-Stokes scattering is shown for completeness of the Raman process.) (B) SERS mechanism, where localized surface plasmons on metallic nanostructures enhance the EM and Raman signal. (C) Schematic of CARS, highlighting the nonlinear four-wave mixing process generating anti-Stokes emission (D) TERS, utilizing a plasmonic metallic tip to confine and enhance the EM field at the nanoscale for high-resolution Raman imaging. (Jones, R.R., Hooper, D.C. Zhang, L. et al. *Raman Techniques: Fundamentals and Frontiers. Nanoscale Res Lett* 14, 231 (2019). 10.1186/s11671-019-3039-2). Adapted from ref 22.

**Table 3. Advantages and Limitations of Raman Spectroscopy and Its Variants, along with A Brief Description and Their Use in Virology, Including Non-Pandemic Viruses**

technique	description	advantages	limitations	refs
Spontaneous Raman	– Inelastic light scattering to capture molecular vibrations	– Nondestructive – Water insensitive	– Weak signal – Fluorescence interference	32
RRS	– Laser tuned to molecular transitions	– Selective enhancement for chromophores	– Not suitable for all molecules	30
SERS	– Nanostructure – Enhanced Raman scattering	– High sensitivity (single-molecule level) – Label-free	– Requires metal substrates – Complex preparation	24,33
TERS	– Raman with scanning probe tip	– Nanoscale spatial resolution	– Requires flat samples – Challenging tip control and its cost	24,26,27,34,35
CARS	– Nonlinear Raman imaging	– Real-time – 3D imaging of live cells	– Complex laser setup	24,25,28
SRS	– Stimulated molecular vibrations with two lasers	– Fast, quantitative chemical imaging	– Expensive, complex instrumentation	24,30

host signaling, with long-read sequencing enabling full-genome analysis and phylogenetic tracking.<sup>14,15</sup> Proteomics and metabolomics, powered by mass spectrometry, reveal host proteome remodeling and metabolic shifts, identifying viral targets.<sup>6,16</sup> Immunological tools like enzyme-linked immunosorbent assay (ELISA), flow cytometry, and immunohistochemistry measure viral load and characterize immune responses.<sup>17,18</sup> Functional assays assess viral entry efficiency, replication kinetics, infectivity, and cell viability under infection or treatment.<sup>7,19</sup> Computational modeling simulates infection, maps host–pathogen networks, and guides therapeutic discovery.<sup>20</sup> Despite their value, these methods face limitations such as low temporal resolution, labeling dependence, and destructiveness, driving interest in label-free, noninvasive techniques like Raman spectroscopy for real-time biochemical monitoring during viral infection.

### Spontaneous Raman Spectroscopy and Its Variants

Raman spectroscopy is a versatile tool for studying virus pathogenesis and virus-host interactions, offering advantages like noninvasiveness, high sensitivity, and molecular specificity. Its molecular vibration-based spectra provide insights into virus behavior with precision.<sup>22,23</sup> Raman spectroscopy has a long history in virus research. Pioneering works in the 1970s–1980s demonstrated that Raman spectra can nondestructively report on viral protein and nucleic-acid organization and discriminate virion types, establishing the conceptual basis for today's SERS/TERS/CARS advances. We now briefly relate current pandemic-virology progress to these foundational demonstrations.<sup>37–40</sup> Before exploring pandemic virus studies, a summary of Raman spectroscopy's principles and features is provided to establish the framework.

Spontaneous Raman spectroscopy provides information on vibrational and low-frequency molecular modes of biomolecules, including proteins, nucleic acids, and lipids, in cellular and biofluid environments. As schematically illustrated in Figure 2A, Raman scattering involves both Stokes and anti-Stokes processes; however, anti-Stokes scattering is rarely exploited in virological applications due to its intrinsically low signal intensity. In both cases, scattering arises from transient, virtual energy states generated during light-matter interaction. The inherently weak Raman signal has therefore motivated the development of enhanced Raman modalities to improve sensitivity and spatial resolution.<sup>22</sup> Table 3 summarizes Raman spectroscopy, its variants, and their advantages and limitations. Several enhanced techniques, including Resonance Raman Spectroscopy (RRS), SERS, and TERS, have been developed to overcome the limitations of spontaneous Raman spectroscopy in terms of weak signal intensity. Briefly, RRS enhances Raman signals by tuning the excitation laser to match an electronic transition of the target molecule, thereby selectively amplifying specific vibrational modes associated with that chromophore. In SERS, incident light excites localized surface plasmons on metallic nanostructures (typically gold or silver), as seen in Figure 2B. This enhances the local electromagnetic (EM) field (illustrated in blue), enhancing the Raman scattering signal through stronger light-analyte interactions near the surface. This approach enables the detection of trace levels of biomolecules and viral components, even at low concentrations, making it especially valuable for sensitive diagnostics and viral detection.<sup>22,24</sup> The relationship between virus and nanoparticle sizes in SERS is crucial. Since many virions (around 50–200 nm) are similar in size to plasmonic nanoparticle assemblies, they can effectively sample multiple hotspots at once, increasing detection chances.<sup>146</sup> However, this size similarity may also cause orientation-dependent enhancement and steric exclusion from narrow gaps, leading to greater spectral variability. To address these challenges, methods such as nanostar<sup>41</sup> or nanoneedle<sup>88</sup> substrates, magnetic enrichment,<sup>38</sup> or shell-isolated particles<sup>64</sup> are used to better control virion placement and enhance detection consistent with the original tone and details reproducibility.<sup>143</sup> TERS combines scanning probe microscopy with Raman spectroscopy to achieve nanoscale spatial resolution. In Figure 2D, TERS leverages a plasmonically active metallic tip that, when illuminated, creates a confined EM field at the tip apex through localized surface plasmon resonance.<sup>22</sup> This intense field (blue) is restricted to the nanoscale region near the tip, significantly enhancing Raman signals from that area. The “lightning rod effect” (curved black arrows) further concentrates the field, enabling chemical imaging with spatial resolution beyond the diffraction limit of conventional optics.<sup>25–27</sup> These enhanced Raman techniques collectively address the sensitivity limitations of spontaneous Raman spectroscopy and open new possibilities for studying virus structure, dynamics, and interactions at unique resolutions. CARS was developed to avoid fluorescence and is a nonlinear technique employing two synchronized lasers. This method can generate high-resolution signals and offers fast imaging capabilities, making it particularly well-suited for live-cell and tissue studies without labeling.<sup>24,28</sup> As shown in Figure 2C, CARS involves a four-wave-mixing process in which synchronized pump and Stokes fields create a (ro-)vibrational coherence, and interaction with the probe field generates the anti-Stokes signal. CARS offers high sensitivity and spatial resolution, making it ideal for imaging live cells and tissues without

labeling.<sup>22</sup> In contrast to the CARS phenomenon, stimulated Raman scattering (SRS) deploys energy, transferring it from incoming photons to the vibrations of molecules.<sup>29</sup> For high-throughput imaging, SRS uses synchronized pump and Stokes beams to amplify vibrational signals and achieve real-time chemical imaging with high sensitivity and minimal background. This technique is useful for studying chromophores and other molecules with strong electronic transitions.<sup>30</sup>

Recent review articles have extensively discussed the potential of Raman spectroscopy and its variants in biomedical diagnostics.<sup>2,24,30,31,142</sup> Orlando et al. emphasized its versatility in detecting diverse biomolecular changes and its broad applications, particularly in virus detection.<sup>31</sup> Another review addressed virion classification, detection, and host immune interactions, highlighting the contribution of advanced biophotonic techniques, including Raman spectroscopy, to viral diagnostics, therapy assessment, and vaccine design.<sup>2</sup> Virus detection may occur through direct identification of viral components such as glycoproteins, nucleocapsids, and genomes, or indirectly by monitoring host responses, including antibodies and cytokines.<sup>30</sup> Changes in body-fluid composition can also indicate infection. At the nanoscale, biochemical signatures are captured through SERS, TERS, and CARS. The incorporation of advanced materials like nanoparticles and carbon nanotubes further strengthens Raman spectroscopy as a rapid, reliable diagnostic platform.<sup>31</sup> Cialla-May et al. reviewed Raman variants for bioanalytical use, focusing on spatial resolution, target size, and sensitivity.<sup>24</sup> Collectively, these studies underline the growing importance of Raman spectroscopy in biomedical diagnostics.

## ■ PANDEMIC VIRUSES' STUDIES BY RAMAN SPECTROSCOPY AND ITS VARIANTS

### Orthomyxoviridae Family

**Influenza Virus.** Single-virion discrimination using TERS on an enveloped influenza A/H1N1 particle and a non-enveloped Coxsackievirus B3 (CVB3) particle was demonstrated by leveraging the nanometer-scale near-field at a metallized AFM tip to obtain highly localized Raman fingerprints.<sup>25</sup> Repeated scans across defined surface areas yielded reproducible TERS spectra and enabled straightforward differentiation between the two virions based on their dominant lipid/protein features for H1N1 versus protein/RNA features for CVB3. Importantly, while the authors discuss CARS and introduce TERS together with CARS (FASTER CARS) as a future route to accelerate acquisition and improve sensitivity, CARS and FASTER CARS spectra shown in the paper are reproduced from an earlier nonviral demonstration<sup>148</sup> rather than measured from virions. Therefore, in the context of virus detection, this study should be cited primarily as a TERS-based single-particle proof-of-capability, with FASTER CARS best framed as a promising development direction for faster nanoscale viral readout, rather than as an established source of viral CARS spectra.<sup>25</sup>

A SERS-based lateral flow assay (SERS-LFA) was developed for rapid detection of influenza A virus, offering improved sensitivity over conventional rapid diagnostic tests.<sup>35</sup> This system enabled highly sensitive and quantitative detection by replacing gold nanoparticles (AuNPs) with Raman-active nano tags. The assay demonstrated a detection limit of  $1.9 \times 10^4$  PFU/mL, ~10-fold more sensitive than colorimetric lateral flow assays, and remained effective at low viral loads. Results were

available within 10 min, combining the simplicity of lateral flow formats with SERS precision for point-of-care influenza diagnostics. Another approach for inactivated H7N9 viruses was established through SERS-coupled lateral flow immunoassay strips (SERS-LFIAS).<sup>37</sup> The system employed core–shell AuAg<sub>4</sub>-ATP@Ag nanoparticles functionalized with H7N9-specific monoclonal antibodies as SERS-active nanotags. The strip contains two capture zones: a test line with H7N9-targeting monoclonal antibodies and a control line containing goat antimouse IgG antibodies for validation purposes. The method has demonstrated high selectivity, with a detection limit (LOD) of 0.0018 hemagglutination units (HAU) for H7N9, validated in spiked cloacal and throat swabs, as well as poultry organs.<sup>37</sup>

In another study, Fe<sub>3</sub>O<sub>4</sub>@Ag magnetic SERS nanotags enabled targeted enrichment of influenza A H1N1 and human adenovirus, improving sensitivity ~2000-fold over colloidal gold-based SERS-LFIA.<sup>38</sup> Anodic aluminum oxide (AAO), with uniform nanopores, was also tested as an alternative to nitrocellulose, improving antigen–antibody interactions in vertical flow assays. Another study developed a rapid quantification method detected multiple respiratory tract infection (RTI) viruses, including IAV, using a 2 × 3 strip encoding 11 nucleic acid targets, achieving LODs of 0.030–0.041 pM and a linear range of 1 pM–50 nM.<sup>39</sup> Another study also explored the use of SERS combined with Principal component analysis (PCA) to identify cells infected with influenza strains A/California/04/2009 H1N1 and A/WSN/33 H1N1, distinguishing viral proteins from host signals.<sup>40</sup> Another group extended intracellular applications by designing DNA hairpin-functionalized gold nanostars for detecting influenza A RNA mutations within HeLa cells at the single-particle level.<sup>41</sup> A magnetic SERS immunosensor was utilized to detect inactivated A(H3N2) by conjugating AuNPs with 4-mercaptobenzoic acid (4-MBA) and influenza A-specific IgG antibodies (AuNPs@4-MBA@IgG).<sup>42</sup> This immunoassay demonstrated an LOD of 10<sup>2</sup> TCID<sub>50</sub>/mL while maintaining high specificity. Viral quantification was performed by monitoring the characteristic Raman peak at 1583 cm<sup>-1</sup> assigned, and the magnetic immunosensor exhibited a linear response across a dynamic range of 10<sup>2–5</sup> × 10<sup>3</sup> TCID<sub>50</sub>/mL. A SERS-enabled aptasensor was designed for detecting multiple IAV subtypes, such as H1, H3, and H5, using DNA aptamers against hemagglutinin, immobilized on silver granules. It achieved an LOD of 1 × 10<sup>-4</sup> HAU per probe.<sup>43</sup> Similarly, in another study, oligonucleotide-based SERS assay was developed for screening indicators of virulence of three wild-type influenza viruses, A/CK/PA/13609/93 (H5N2) (No mutation), A/Mute Swan/MS451072/06(H5N1) (N66S mutation) and A/CK/TX/167280–04/02 (H5N3) (N66S mutation).<sup>44</sup> These mutations are linked to increased virulence in strains such as the 1918 H1N1 and 1997 H5N1 viruses. The study developed a SERS assay by immobilizing 5'-thiol-modified ssDNA probes onto silver nanorod substrates, targeting conserved PB1-F2 gene sequences. Spacer molecules minimized nonspecific binding, enabling precise hybridization and enhancing assay sensitivity for detecting virulence determinants. A label-free virus detection method used sodium borohydride-reduced AgNPs to eliminate background from citrate-reduced substrates and improve viral protein binding.<sup>45</sup> It detected SARS-CoV-2, human adenovirus 7, and H1N1 in PBS, serum, and saliva within 2 min, reaching 10 copies/test, with LDA classifying viruses by distinct SERS fingerprints. A related study using commercial SERS substrates and purified A(H1N1)-pdm09 and B/Hong Kong/269/2017 viruses showed similar

results.<sup>46</sup> SERS combined with a support vector machine (SVM) model classified influenza A and B with 93% accuracy, maintaining 84% at 0.05 μg/mL. In another study, digital microfluidic SERS was employed to quantitatively detect the avian virus H5N1. This method offers a sensitivity of 74 pg/mL, a detection time under 1 h, and uses notably less reagent (30 μL) than the standard ELISA.<sup>149</sup> SERS also enabled detection of Tamiflu-resistant influenza in nasal fluid and saliva. Distinct vibrational spectra differentiated resistant from nonresistant strains, confirming SERS as a fast, real-time tool for antiviral resistance detection.<sup>47</sup> In a review, SERS-based diagnostic strategies, evaluating sensitivity, mechanism, and point-of-care potential for respiratory viruses, were summarized.<sup>48</sup>

### Filoviridae Family

**Marburg Virus (MARV).** Research on detecting and analyzing *Filoviridae* family, including MARV and Ebola, using Raman spectroscopy is still in its early stages. Direct Raman studies on MARV are limited, but progress has been made with Raman-based biosensing systems for detecting virus-sized particles and airborne viruses. The most relevant studies below outline advances offering insight into Raman use for viral detection. One study developed a SERS platform with a metal–insulator–metal nanostructure that distinguished MARV from other viruses (Influenza A, Zika, and Coronavirus) using PCA for spectral visualization and a random forest model for classification.<sup>49</sup> MARV showed distinct Raman fingerprints, achieving 83–95% accuracy and proving high sensitivity and specificity for complex, enveloped viruses. When grouped with Zika as “non-respiratory viruses,” the model reached 99% binary accuracy in separating them from respiratory pathogens. Another study discussed in the Influenza section also showed the cross-applicability of this Raman-PCA approach to MARV.<sup>46</sup>

**Ebola Virus.** A single study has reported the use of Raman spectroscopy for Ebola virus detection.<sup>50</sup> It emphasized the major challenges in diagnosing and managing Ebola, mainly the lack of affordable, field-deployable tools and the similarity of early symptoms to other diseases such as malaria. The study introduced a SERS-based immunoassay capable of detecting Ebola, Lassa fever, and malaria antigens from a single blood sample within 30 min. It achieved 90% sensitivity and 97.9% specificity for Ebola, and 100% sensitivity and 99.6% specificity for malaria, using clinical samples from the 2014 West African Ebola outbreak. These findings demonstrate the potential of SERS technology for possible rapid outbreak detection and clinical triage in resource-limited regions.

### Flaviviridae Family

**Dengue Virus (DENV).** A SERS-hybridization chain reaction (HCR) platform was developed for the ultrasensitive DENV gene detection in a study.<sup>51</sup> It combines localized catalytic hairpin assembly (LCHA) with HCR to amplify signals, which are then transferred onto Ag nanorod (AgNR) arrays for SERS readout. The assay achieved a linear range of 1 fM–10 nM with a LOD of 0.49 fM, offering ~5-fold higher signal-to-noise and ~4.5-fold greater sensitivity than traditional CHA. Ngo et al. further developed a DNA bioassay-on-chip using a bimetallic nanowave chip, enabling direct SERS readout without washing steps and successfully detecting DENV-4 sequences.<sup>52</sup>

Detection of DENV in whole blood and serum specimens with 532 nm excitation has also been employed to identify antibody (IgG and IgM, related peaks 1614, 1750 cm<sup>-1</sup>, respectively) and ADP release markers (750, 850 cm<sup>-1</sup>).<sup>53</sup> The spectra also exhibited a characteristic cortisone peak at 1732

$\text{cm}^{-1}$ , while showing depletion of carotenoid-associated bands (1006, 1156, and  $1516\text{ cm}^{-1}$ ) in infected samples. A quantitative model was developed and validated to screen IgG-positive human sera for DENV using 79 samples, yielding an R-squared value of 0.91. This model revealed molecular changes associated with IgG, showing positive correlations with myristic acid and negative correlations with collagen, demonstrating high accuracy and agreement with clinical data.<sup>53</sup> In another study, blood from 40 DENV-positive patients and 25 controls was analyzed to link ADP peaks to the rupturing of thrombocytes, a consequence of DENV infection.<sup>54</sup> Characteristic biochemical alterations associated with dengue infection were identified, particularly through distinct vibrational modes at 750 and  $850\text{ cm}^{-1}$  corresponding to ADP biomarkers. The study highlights the potential of Raman spectroscopy as a rapid, noninvasive method for monitoring dengue infection and recovery.<sup>55</sup> The same group also explored Raman spectroscopy combined with SVM for diagnosing dengue infection through human blood serum analysis. The study involved 84 samples (31 dengue-positive, 53 negative) collected from suspected patients, with Raman spectra acquired in the  $600\text{--}1700\text{ cm}^{-1}$  range. Distinct spectral differences were observed between infected and healthy samples, including suppressed peaks at 1003, 1156, and  $1516\text{ cm}^{-1}$  and additional peaks at 750, 850, 1450, and  $1660\text{ cm}^{-1}$  (Table 4), in dengue cases. Various SVM kernels were tested, with the polynomial kernel (order 1) achieving the best performance: 85% accuracy, 90% precision, 73% sensitivity, and 93% specificity. In a study of the same group evaluating the diagnostic power of Raman spectroscopy combined with machine learning, blood serum samples from 100 individuals suspected of dengue fever were analyzed, 45 of which were IgM-positive based on ELISA testing.<sup>56</sup> Using a 532 nm laser-based Raman spectrometer, spectra were acquired from dried serum drops and processed to remove background fluorescence. Distinct spectral changes in dengue-positive samples included suppressed  $\beta$ -carotene peaks ( $1156, 1516\text{ cm}^{-1}$ ) and the emergence of lactate-related peaks ( $750, 830, 1123, 1448, 1660\text{ cm}^{-1}$ ), reflecting biochemical alterations due to infection. PCA was used for dimensionality reduction, followed by classification using a Random Forest (RF) model. The system achieved 91% sensitivity, specificity, and accuracy on both full and test subsets, demonstrating strong performance compared to standard ELISA assays. A label-free Raman spectroscopy-based method was developed for rapid screening of dengue infections using human blood plasma, identifying elevated lipid ( $608, 875, 1297, 1719, 1736\text{ cm}^{-1}$ ) and protein ( $1239, 1507, 1540, 1640, 1680\text{ cm}^{-1}$ ) markers in infected samples.<sup>57</sup> Multivariate analysis using Principal Component Analysis and Factorial Discriminant Analysis (PCA-FDA) achieved a sensitivity of 98% and specificity of 95% in distinguishing infected samples. In another study, 785 nm laser was used to differentiate dengue infection from typhoid infection in 62 human serum samples (31 per group).<sup>58</sup> A distinct  $1686\text{ cm}^{-1}$  band, attributed to soluble ST2 protein, marked DENV infection, while other biomarkers differentiated typhoid. Raman spectroscopy combined with PLS regression was used to detect the molecular alterations associated with early stage DENV infection via NS1 protein, detectable 3 days post-infection.<sup>59</sup> In 39 serum samples, cytokines ( $775\text{--}875\text{ cm}^{-1}$ ), lectins ( $1003\text{--}1672\text{ cm}^{-1}$ ), DNA ( $1040\text{--}1140\text{ cm}^{-1}$ ), and protein structures ( $933\text{--}967\text{ cm}^{-1}$ ) were identified as key markers. The model achieved an  $R^2$  of 0.891 and 100% sensitivity, specificity, and accuracy, confirming its strong

**Table 4. Representative Raman Bands Associated with Virion Components and Host-response Biomarkers**<sup>11,22,32,40,49,53–55,57,65,81,85,97,145a</sup>

Raman shift ( $\text{cm}^{-1}$ )	assignment	interpretation
~488	Disulfide bond (S–S stretching)	Protein tertiary structure
~636	N-acetyl glucosamine/phenyl ring	Glycoprotein-associated signatures
~720–735	Adenine ring breathing	Viral genome presence; increased host transcription
~780–785	Cytosine/uracil ring breathing	Viral nucleic acid fingerprint
~830–850	Tyrosine residues	Immune signaling, phosphorylation
~860	Nucleic acids/phosphodiester	Genome/backbone-associated signatures in infection
~892	Deoxyribose (in-plane mode)	Nucleic-acid-associated changes
~940–960	Protein backbone ( $\alpha$ -helix)	Conformational protein changes
~1000–1006	Phenylalanine	Structural proteins; total protein content
~1080–1100	$\text{PO}_2^-$ stretching	Membrane remodeling during replication
~1120–1130	C–C stretching of lipids/proteins	Enveloped virus identification
~1156	C–C stretch mode of $\beta$ -carotene	Carotenoid depletion associated with viral infection
~1200–1210	Tryptophan/Amide III	Protein/aromatic amino-acid changes; infection signature
~1240–1270	Amide III $\beta$	Protein secondary structure changes
~1330–1360	CH deformation/nucleic acids	Metabolic activation; RNA/protein overlap
~1425–1450	$\text{CH}_2/\text{CH}_3$ deformation	Lipid metabolism alteration
~1516	$\beta$ -carotene (C = C stretching)	Carotenoid depletion associated with viral infection
~1520–1560	Amide II/aromatic residues	Viral protein composition; variant effects
~1570–1610	Tryptophan	Protein-associated changes
~1650–1665	Amide I	Protein folding, inflammation
~1730–1750	C = O ester stretches	Lipid oxidation, membrane damage
~2850–3000	C–H stretching (lipids/proteins)	Membrane remodeling/lipid-protein content

<sup>a</sup>Band positions may shift depending on excitation wavelength, enhancement strategy, and local chemical environment.

diagnostic potential.<sup>59</sup> In another study, PCA was applied to extract NS1 features from SERS spectra of NS1-adulterated saliva samples, revealing a characteristic NS1 peak at  $\sim 1000\text{ cm}^{-1}$  and reducing data dimensionality by >90% while preserving key features.<sup>60</sup> PCA score plots clearly separated NS1-positive from healthy samples, highlighting the potential for a rapid, noninvasive SERS-based classification method for dengue diagnosis.<sup>60</sup> The same group analyzed salivary SERS spectra from suspected dengue patients and the control group using PCA.<sup>61</sup> PCA were statistically tested, with significant differences observed between NS1-positive and negative samples in both ELISA (PC1, PC2) and rapid test data sets (PC1, PC3, PC5). These PCs may serve as effective inputs for classifying NS1 in saliva, supporting noninvasive dengue diagnosis.<sup>61</sup> By analyzing Raman spectral features, they identified viral RNA with a sensitivity of  $7.05 \times 10^7$  transduction units per mL. The study represents a preliminary step toward using noninvasive saliva sampling for viral detection. Other research group utilized Raman spectral data to observe

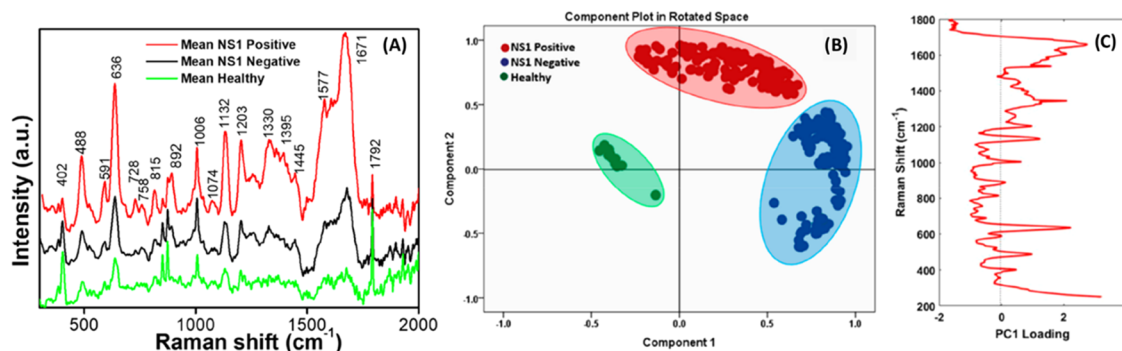


**Figure 3.** (A) Mean SERS spectra of NS1-positive dengue samples, NS1-negative febrile controls, and healthy individuals, highlighting distinct biochemical signatures. (B) PCA score plot showing clear separation of the three groups based on SERS spectral features. (C) PC1 loading plot indicating Raman bands contributing most strongly to classification. (Gahlaut, S. K.; Savargaonkar, D.; Sharan, C.; Yadav, Sarjana, Mishra, P.; Singh, J. P. *SERS Platform for Dengue Diagnosis from Clinical Samples Employing a Hand Held Raman Spectrometer*. *Anal. Chem.* **2020**, *92* (3), 2527–2534. [10.1021/acs.analchem.9b04129](https://doi.org/10.1021/acs.analchem.9b04129)) Adapted from ref 145.

molecular changes associated with viral RNA, focusing on specific spectral signatures that differentiate between infected and uninfected samples.<sup>62</sup> A field-deployable SERS platform employing silver nanorod arrays and a hand-held Raman spectrometer has also been demonstrated for early stage dengue diagnosis directly from clinical serum samples using silver AgNR substrates and PCA-based chemometric analysis.<sup>145</sup> As illustrated in Figure 3A, mean SERS spectra revealed distinct biochemical differences among NS1 positive, NS1 negative, and healthy samples, with characteristic bands at  $\sim 488\text{ cm}^{-1}$  (disulfide bonds),  $728\text{ cm}^{-1}$  (adenine), and  $892\text{ cm}^{-1}$  (deoxyribose), indicating nucleic-acid- and protein-related changes associated with infection. Additional bands at  $1006\text{--}1132\text{ cm}^{-1}$  (phenylalanine and lipid-related modes, see Table 4) and in the amide regions ( $1203$ ,  $1577$ , and  $1671\text{ cm}^{-1}$ ) reflect alterations in protein composition and secondary structure. As seen in Figure 3B, PCA clearly separated the three groups in the reduced feature space, highlighting the discriminatory power of SERS-based molecular fingerprints for dengue infection. The corresponding PC1 loading plot identified the Raman shifts contributing most strongly to class separation, confirming that biochemical alterations dominate the spectral variance (Figure 3C). This study demonstrates label-free dengue screening using portable SERS instrumentation combined with chemometric analysis, supporting its potential for point-of-care diagnostics.

**Zika Virus.** A study discusses showcasing a SERS-based immunoassay capable of distinguishing between Zika and DENV viral biomarkers with high sensitivity.<sup>63</sup> This study utilized Au nanostars conjugated to specific antibodies for Zika and Dengue NS1. The SERS-based assay demonstrated significantly lower detection limits compared to traditional LFIA, with a 15-fold improvement for Zika NS1 and a 7-fold improvement for Dengue NS1. As seen in Figure 4A–C, the samples tested include a control (0 ng/mL NS1, gray), Zika NS1 (blue), Dengue NS1 (cyan), and a mixture of Zika and Dengue NS1 (yellow). Each spectrum represents the average of 10 measurements for each spot. This platform combines the simplicity of LFAs with the enhanced sensitivity of SERS, making it ideal for rapid, point-of-care diagnostics in resource-poor settings.<sup>63</sup> The study aims to overcome the limitations of traditional diagnostic methods, which face challenges due to low levels of Zika biomarkers in the blood and the frequent cross-reactivity with other flaviviruses such as DENV.<sup>64</sup> To address these issues, the researchers designed Au shell-isolated nanoparticles (Au-SHINs) coated with a Raman reporter (Nile Blue)

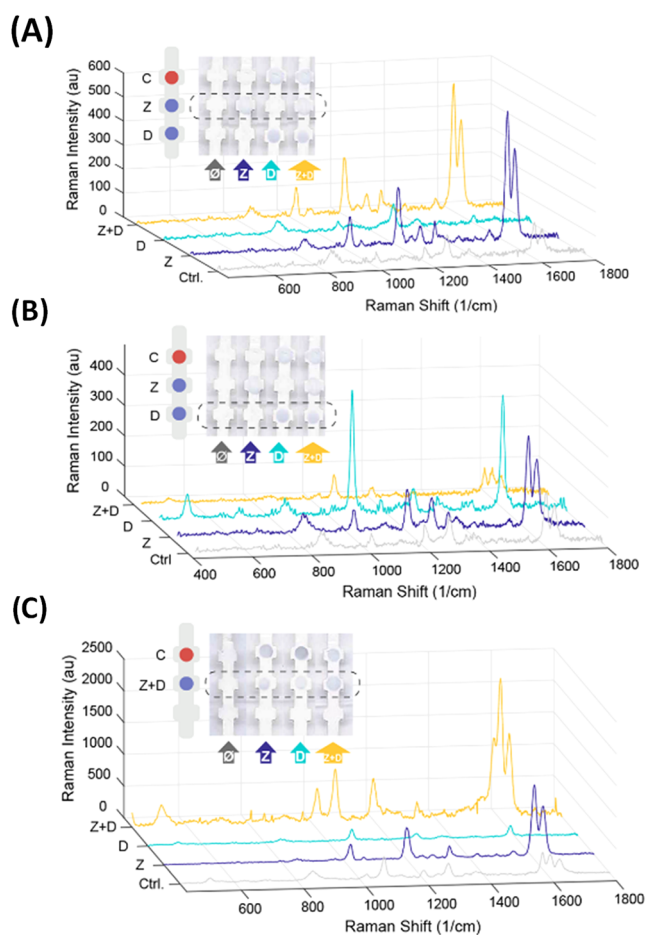


**Figure 4.** Multiplexed SERS assay where Zika and Dengue test lines are separately painted. SERS spectra are shown for Zika (A) and Dengue (B) test lines and a combined Zika-Dengue test line (C). (Sánchez-Purrà M, Carré-Camps M, de Puig H, Bosch I, Gehrke L, Hamad-Schifferli K. (2017) *Surface-Enhanced Raman Spectroscopy-Based Sandwich Immunoassays for Multiplexed Detection of Zika and Dengue Viral Biomarkers*. *ACS Infect Dis.*;3(10):767–776. doi: [10.1021/acsinfectdis.7b00110](https://doi.org/10.1021/acsinfectdis.7b00110)). Adapted from ref 63.

and surrounded by a silica shell, which were then functionalized with monoclonal antibodies specific to Zika virus NS1 antigens. This immunoassay demonstrated the ability to detect Zika NS1 antigen at concentrations as low as 10 ng/mL, with no cross-

reactivity to DENV NS1 antigens, a significant improvement over existing methods that often result in false positives. The assay detects Zika antigens by measuring Raman signals from Nile Blue reporters on functionalized nanoprobe. It showed markedly higher sensitivity and specificity than ELISA, with reduced cross-reactivity, highlighting its potential for early Zika diagnosis in outbreak settings.<sup>64</sup> A biosensor using SERS was developed for rapid and sensitive detection of the Zika virus, utilizing silver nanoislands (AgNIs) as the active platform.<sup>65</sup> The AgNIs were thermally deposited on glass coverslips and functionalized with anti-Zika antibodies, enabling the detection of viral antigens at concentrations as low as 0.11 ng/mL. The biosensor demonstrated a strong, linear Raman response between 5 and 1000 ng/mL, particularly evident at the 1570  $\text{cm}^{-1}$  peak corresponding to tryptophan within the protein-associated region highlighted in Table 4. Offering advantages in speed, cost-efficiency, and low sample volume, this method addresses challenges of low viral load in early stage infections.

### Picornaviridae Family

**Echovirus.** A single study has been identified that investigates the molecular dynamics associated with the uncoating process of Echovirus 1 (EV1) using Raman spectroscopy.<sup>11</sup> The researchers utilized a 532 nm laser with a power output of 25 mW to record the Raman spectra of EV1 samples both in vitro and in cell cultures to mimic in vivo conditions. Distinct Raman markers differentiated intact, intermediate, and disrupted particles, revealing reduced  $\alpha$ -helix and increased  $\beta$ -sheet/coil content, shifts in tryptophan/tyrosine environments, and RNA conformational changes during genome release. Using a 532 nm laser (25 mW, 10 s acquisition), spectra were recorded from EV1 both in vitro and in cell culture to mimic in vivo conditions. Additional signatures indicated salt bridge cleavage and fatty acid release, consistent with known uncoating mechanisms. This work highlights Raman spectroscopy's capacity to track viral protein sensitively and RNA rearrangements during uncoating, complementing conventional structural approaches.

**Poliovirus.** Although direct Raman studies on poliovirus are lacking, Silge et al. demonstrated the feasibility of identifying IPV-containing combination vaccines using drop-coating deposition Raman spectroscopy (DCDRS).<sup>66</sup> Commercial Diphtheria, Tetanus, acellular Pertussis & Inactivated Poliovirus (DTaP-IPV) formulations produced distinct spectra due to their antigenic and adjuvant compositions ( $\text{Al}(\text{OH})_3$  or  $\text{AlPO}_4$ ), enabling PCA-LDA classification with up to 100% specificity and sensitivity of various vaccine products, including those containing IPV components. These results highlight Raman spectroscopy's potential as a quality control and anticounterfeiting tool for poliovirus vaccines and suggest future applications in IPV antigen characterization and formulation monitoring, while circumventing biosafety constraints of live virus handling.<sup>66</sup> The absence of Raman studies on poliovirus, despite its clinical importance, likely reflects strict biosafety regulations under the Global Polio Eradication Initiative,<sup>67</sup> the long-standing availability of effective vaccines and diagnostics, and the virus's small, nonenveloped structure that produces weak Raman signatures. Existing data, mostly from inactivated samples or model systems, remain limited in technical and clinical depth.

### Poxviridae Family

**Smallpox Virus.** Limited research has been conducted on this virus family, similar to the Picornaviridae family. Therefore, the study conducted in 2008 appears to be the only research on

the smallpox virus.<sup>68</sup> In this study, SERS was developed for the rapid discrimination of various species of Poxviridae viruses, specifically bovine papular stomatitis virus (BPSV), pseudocowpox virus (PCPV), and Yaba monkey tumor virus (YMTV), which are taxonomically close to smallpox. The study utilized commercial-off-the-shelf (COTS) SERS-active substrates, which provide reproducible and spatially uniform surfaces for enhanced Raman signal acquisition, combining with PLS2-based chemometric models that could accurately classify viral species based on their unique SERS spectral signatures. The study demonstrated a high specificity of the methodology, with no false negatives and only a small ( $\sim 10\%$ ) false positive rate during the classification of viral samples. The spectral analysis reveals prominent viral peaks located at approximately 455, 853, 1003, and 1168  $\text{cm}^{-1}$ . While the Raman signatures of BPSV and PCPV exhibit considerable overlap, distinctive vibrational modes at 539, 853, and 1168  $\text{cm}^{-1}$  are uniquely present in the BPSV spectrum but absent in PCPV. This implies that it is possible to distinguish between BPSV and PCPV based on their molecular composition and SERS spectral signatures. This work represents the first instance of using COTS SERS substrates to discriminate intact poxviruses without the need for molecular recognition elements, marking a significant step forward in biosensing and diagnostic technology.<sup>69</sup>

**Monkeypox Virus (MPXV).** In a study, a method for detecting MPXV protein and nucleic acid to overcome biosafety restrictions was developed using calcium ions to reduce signal interference and enhance SERS signals.<sup>70</sup> The method can detect MPXV protein at 5 ng/mL and nucleic acid at 100 copies/mL in under 2 min, offering a faster alternative to PCR. It also distinguishes different proteins in serum and shows potential for quantitative virus detection using SERS. A study develops a dual-mode immunochromatographic assay (ICA) using colorimetric and SERS for MPXV detection. It uses molybdenum disulfide ( $\text{MoS}_2$ ) nanosheets loaded with multi-layered AuNPs, enhanced with a polyethylenimine (PEI) interlayer for better detection in complex samples.<sup>71</sup> Targeting the MPXV A29L protein, it detects the virus in biological and environmental samples at as low as 0.2 ng/mL (colorimetric) and 0.002 ng/mL (SERS), offering improved sensitivity over PCR and ELISA.<sup>71</sup> Another study focuses on developing a label-free virus detection method based on SERS to detect MPXV and human papillomavirus (HPV) using AgNPs synthesized through sodium borohydride reduction to minimize background interference from biological sample, such as serum (100 MPXV groups) and artificial vaginal (100 HPV groups) discharge.<sup>72</sup> Tested in serum and artificial vaginal discharge, the approach achieved a detection limit of 100 copies/mL with good reproducibility. PCA enabled clear viral discrimination, demonstrating rapid, sensitive, and selective detection in complex biological samples without the need for labeling.

### Nairoviridae Family

**Crimean-Congo Hemorrhagic Fever Virus (CCHF).** Although CCHFV is a high-priority virus, no Raman spectroscopy studies have been reported. Research is limited by the strict biosafety requirements for handling this highly infectious virus with a high fatality rate and nosocomial risk.<sup>73</sup> Such conditions restrict access and make Raman systems unsuitable for BSL-4 laboratories. The sporadic outbreaks, mainly in low-resource regions of Africa, Asia, and Eastern Europe, further reduce sample availability and investment interest in Raman diagnostics. Thus, current detection relies on nucleic acid

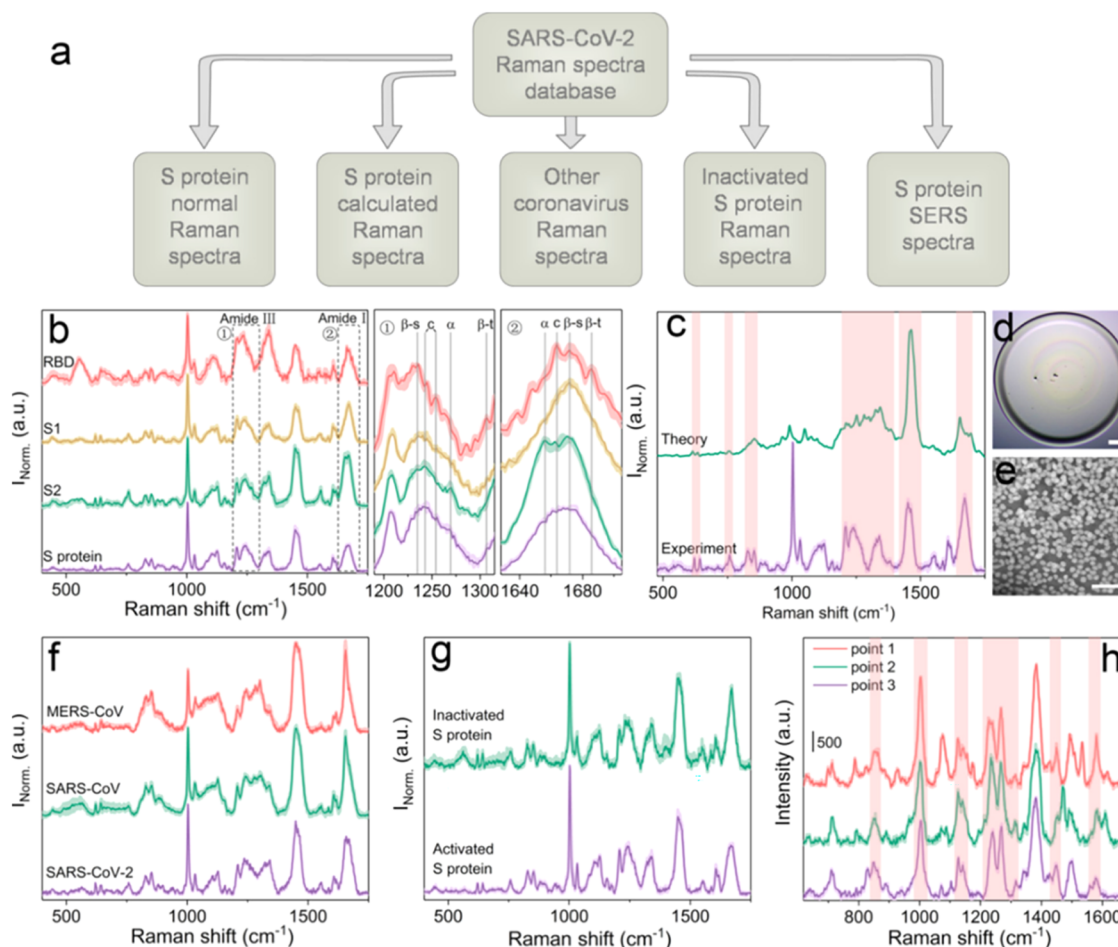


**Figure 5.** Development of a Raman spectral database for the SARS-CoV-2 spike protein. (a) Schematic overview illustrating the structural organization of the spectral database. (b) Standard Raman spectra obtained for the full-length spike (S) protein, its subunits S1 and S2, and RBD. (c) Comparative analysis between computed and experimentally recorded Raman spectra for the S1 subunit. (d) Optical image of the S protein dried on a silver-coated silicon substrate; scale bar: 300  $\mu\text{m}$ . (e) Scanning electron microscopy image depicting the Au nanoparticle array used for SERS measurements; scale bar: 200 nm. (f) Comparative Raman profiles of the spike proteins from SARS-CoV-2, SARS-CoV, and MERS-CoV, expressed in insect cells using the baculovirus system. (g) Raman spectral differences in SARS-CoV-2 S protein before and after thermal treatment. (h) SERS spectra of the SARS-CoV-2 spike protein. (Huang, J., Wen, J., Zhou, M., Ni, S., Le, W., Chen, G., Wei, L., Zeng, Y., Qi, D., Pan, M., Xu, J., Wu, Y., Li, Z., Feng, Y., Zhao, Z., He, Z., Li, B., Zhao, S., Zhang, B., Xue, P., He, S., Fang, K., Zhao, Y., & Du, K. (2021). On-site detection of SARS-CoV-2 antigen by deep learning-based surface-enhanced Raman spectroscopy and its biochemical foundations. *Analytical Chemistry*, 93(26), 9174–9182.) (Adapted from *Analytical Chemistry*, 2021, 93, 9174–9182). Reprinted from ref 87.

amplification and serological assays, which remain the established standard.

### Arenaviridae Family

**Lassa Virus.** The Lassa virus, a BSL-4 virus endemic to West Africa,<sup>74</sup> has not been studied using Raman spectroscopy for detection or research like CCHF. This gap stems from biosafety and logistical barriers, as high-containment laboratories typically lack Raman or SERS equipment. Clinically, Lassa fever mimics other febrile illnesses such as malaria and typhoid,<sup>74</sup> complicating the identification of specific vibrational biomarkers. Progress is further limited by funding constraints, restricted access to well-characterized samples, and reliance on established diagnostics like RT-PCR and lateral flow assays. Unless portable, closed-system Raman devices or suitable surrogate models become available, the application of Raman spectroscopy to Lassa virus research will likely remain constrained.

### Coronaviridae Family

**SARS-CoV-2.** The COVID-19 pandemic has profoundly affected billions of people globally, highlighting the urgent need for rapid, effective, and cost-efficient diagnostic tools for this virus and potential future outbreaks.<sup>75</sup> In response to this challenge, researchers have proposed innovative diagnostic technologies that utilize Raman spectroscopy and its variants, combined with advanced computational methods, for rapid, accurate virus detection across a range of body fluids and infected cells. Spontaneous Raman spectroscopy with a 785 nm laser and a 30-s integration time was employed to diagnose COVID-19 in human serum samples.<sup>76</sup> Spectra from positive and negative individuals were analyzed using PCA and PLS-Discriminant Analysis (DA), revealing molecular markers linked to immune response and viral presence. In the context of COVID-19, a SERS platform based on Au/Ag nanostructures sputtered onto silicon nanorods was developed for the detection of the SARS-CoV-2 receptor-binding domain (RBD), achieving detection limits as low as 1 pM with high specificity confirmed

through antibody-functionalization.<sup>77</sup> In another study, a method for detecting coronavirus infections was developed by analyzing human serum using Raman spectroscopy and a machine-learning-based SVM to build a database of spectral fingerprints.<sup>78</sup> Another group developed a SERS-based point-of-care tool in order to distinguish SARS-CoV-2-positive and negative samples from saliva and nasopharyngeal swab.<sup>79</sup> Saliva proved more reliable, exhibiting significant biochemical changes, including increased levels of methionine, nucleic acids, ferritin, and immunoglobulins, thereby improving diagnostic accuracy. The representative nucleic-acid and protein band regions are summarized in Table 4. Using chemometric analysis, the SVMC model achieved 100% calibration accuracy. The study also highlighted neopterin in swabs sample as a potential biomarker for early immune response and disease severity. Furthermore, in another study, analyzing dried saliva droplets with multiple instance learning achieved an AUC of 0.8, with sensitivity/specificity of 79%/75% in males and 84%/64% in females.<sup>80</sup> Incorporating donor sex improved model performance, underscoring the role of biological variability in saliva-based diagnostics. Further highlighting subcellular-level analysis, Raman spectral features from nucleolar regions of lung cells provided the most discriminative information between healthy and cancerous cells.<sup>81</sup> Shifting to COVID-19 diagnostics, Raman spectroscopy was applied to nasopharyngeal swabs samples, achieving 91% diagnostic accuracy using PCA and PLS-DA, effectively differentiating infected individuals from healthy controls.<sup>82</sup> In another study, serum immunoglobulin markers were analyzed using a dispersive Raman setup, noting biochemical signatures of COVID-19, including decreased albumin and increased lipids and nucleic acids.<sup>83</sup> Rapid, portable detection solutions were also advanced by developing a one-step aptamer-based SERS assay targeting the SARS-CoV-2 spike protein, detecting pseudoviruses within 5 min without sample pretreatment.<sup>84</sup> Using a hand-held Raman spectrometer (785 nm excitation), the method achieved a LOD of 124 TU/ $\mu$ L, contributing to variant identification by introducing the concept of a Raman barcode. Using high-resolution Raman spectra collected from original and British SARS-CoV-2 variants in Japan, they identified differences in sulfur-containing amino acid rotamers, RNA components, and protein structures.<sup>85</sup> Label-free SERS strategies were further explored by applying a portable 532 nm Raman setup to nasal swab samples from 75 positive and 75 negative individuals.<sup>86</sup> After data preprocessing with smoothing and baseline correction, specific Raman peaks associated with proteins, lipids, and glycoproteins allowed differentiation with minimal false positives. For influenza virus detection, a sandwich immunomagnetic bead SERS system targets H5N1 influenza. Utilizing a 532 nm laser with *in situ* AgNPs synthesis, it achieves a detection limit of  $5.0 \times 10^{-6}$  TCID50/mL, with 100% specificity.<sup>35</sup> A residual neural network-based model to assist SERS analysis was used to detect SARS-CoV-2 antigen in pharyngeal swabs or sputum of COVID-19 patients for the rapid on-site diagnosis of SARS-CoV-2.<sup>87</sup> As seen in Figure 5, Raman spectra database of the S protein of SARS-CoV-2, including the architecture of the spectra database and Normal Raman spectra of the S protein, the S1 subunit, the S2 subunit, and the RBD of SARS-CoV-2 was obtained. Furthermore, the theoretical and experimental Raman spectra of the S proteins of SARS-CoV-2, SARS-CoV, and Middle East respiratory syndrome coronavirus (MERS-CoV), expressed in baculovirus-infected insect cells, were compared. As a result, the method has exhibited a diagnostic accuracy of

87.7%, establishing its potential as a promising approach for expediting on-site diagnosis of SARS-CoV-2.

In another study, a SERS biosensor was developed based on plasma-engineered 3D silver nano assemblies on cellulose paper.<sup>89</sup> Functionalized with variant-specific antibodies, their system detected SARS-CoV-2 spike and nucleocapsid proteins, including wild-type,  $\alpha$ , Delta, and Omicron variants, in artificial saliva, with detection limits as low as 1 fg/mL for spike protein and 0.1 pg/mL for nucleocapsid protein. The SERS combined with artificial intelligence enables the swift detection and classification of respiratory viruses such as SARS-CoV-2, hCoV-229E, and Influenza A H1N1 by culturing in Vero-E6, MRC-5, and MDCK cells, respectively.<sup>90</sup> Using standardized protocols across different viral cultures, the study analyzed 20 hCoV-229E, 24 SARS-CoV-2, and 46 H1N1 samples.<sup>90</sup> Average SERS spectra for the three viruses are displayed with distinct vibrational bands, including those at 659, 734, 755, 860, 1123, 1352, 1430, 1535, and 1564  $\text{cm}^{-1}$ , several of these fall within the nucleic-acid ( $\sim 720\text{--}785 \text{ cm}^{-1}$ ), lipid ( $\sim 1440\text{--}1450 \text{ cm}^{-1}$ ), and protein (amide/aromatic) regions summarized in Table 4, which characterize the biomolecular fingerprints of the viral samples. Spectral regions show biochemical signatures across all three viruses, which may correspond to shared protein or nucleic acid components. The model achieved high accuracy in distinguishing negative samples from three respiratory viruses.

The study evaluates SERS-LFIAS approach to enhance detection capabilities using samples from HPV and influenza virus.<sup>91</sup> The SERS-LFIAS approach demonstrated significant improvements in sensitivity and specificity compared to conventional LFIAS.<sup>91</sup> Another group integrated SERS with LFIAs for simultaneous detection of SARS-CoV-2 IgM and IgG.<sup>92</sup> Using  $\text{SiO}_2@$ Ag-spike (S) protein nanoprobe and a portable Raman reader, the assay achieved a detection limit 800-fold lower than conventional AuNP-based LFIAs and showed strong performance with 19 positive and 49 negative serum samples. In another study, a vertical flow assay platform was developed for enabling the simultaneous SERS-based detection of SARS-CoV-2 and influenza A virus.<sup>93</sup> The method utilized Au@AgNBA@Au and Au@AgMB@Au nanoparticle-based SERS nanotags, each functionalized with virus-specific antibodies, to form distinct sandwich immunocomplexes upon binding with target antigens on anodic AAO substrates. The assay achieved impressive limits of detection: 0.47 pg/mL for SARS-CoV-2 and 0.62 pg/mL for influenza A virus. A SERS-ELISA was also created in another study, which allows high-sensitivity screening of multiple patient samples on a 1536-well plate.<sup>94</sup> Increasing the well number from 96 to 1536 boosts throughput but reduces sensitivity due to fewer biomarkers and more nonspecific binding. To improve sensitivity,  $\text{SiO}_2$  beads were used to increase the surface area and biomarker loading. Using a 3D AuNP@ $\text{SiO}_2$  SERS platform, LOD for SARS-CoV-2 nucleocapsid protein dropped from 273 to 7.83 PFU/mL, compared to a 2D AuNP platform. This AuNPs@ $\text{SiO}_2$  SERS immunoassay (SERS-IA) could significantly reduce false negatives in current LFAs or ELISAs by detecting low virus concentrations. Another study focused on a sensitive and flexible SERS-based sensing platform for detecting COVID-19. This platform utilized flexible SERS substrates to provide ultra-responsive detection methods, which are crucial for real-world applications.<sup>95</sup> Another group utilized a plasmonic syringe filter combined with SERS to develop a rapid detection system for biomarkers.<sup>96</sup> The system was tested using human IgG as a model diagnostic biomarker, demonstrating rapid, sensitive, and

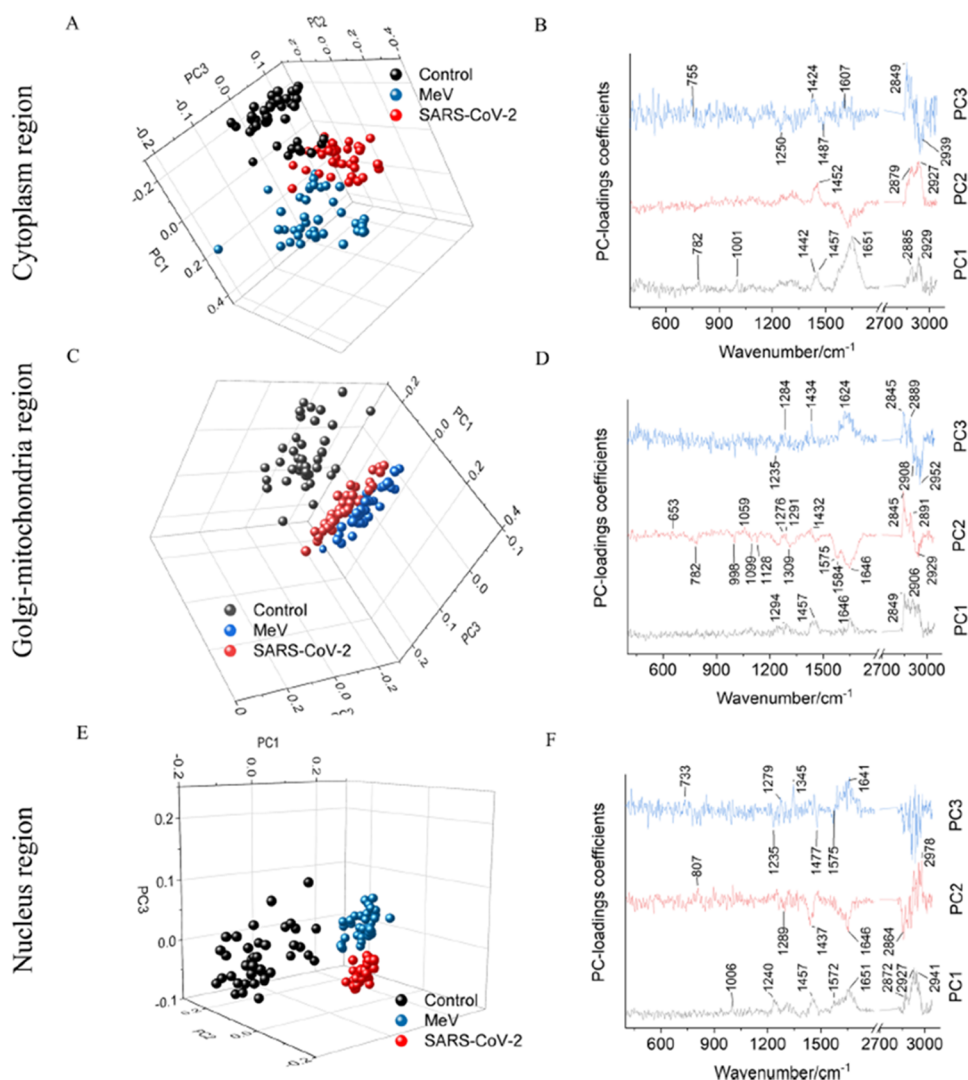


**Figure 6.** (A) PCA of confocal Raman spectra extracted from intracellular compartments of Control, measles virus (MeV)-infected, and SARS-CoV-2-infected Vero E6 cells. (A, B) Cytoplasm region: (A) 3D PCA score plot and (B) corresponding PC loadings. (C, D) Golgi-mitochondria region: (C) PCA score plot and (D) PC loadings. (E, F) Nucleus region: (E) PCA score plot and (F) PC loadings. (Salehi, H.; Ramoji, A.; Mougari, S.; Merida, P.; Neyret, A.; Popp, J.; Horvat, B.; Muriaux, D.; Cuisinier, F. *Specific intracellular signature of SARS-CoV-2 infection using confocal Raman microscopy. Commun Chem* 2022, 5 (1), 85. DOI: 10.1038/s42004-022-00702-7.) Reprinted from ref 97.

quantitative detection capabilities. Another study demonstrates that confocal Raman microscopy can effectively detect specific changes within cells caused by SARS-CoV-2, the virus responsible for COVID-19.<sup>97</sup> As illustrated in Figure 6A,C,E, PCA of Raman spectra extracted from distinct subcellular compartments (cytoplasm, Golgi-mitochondria region, and nucleus) enables clear separation of noninfected, MeV-infected, and SARS-CoV-2-infected cells. The corresponding PC loading plots (Figure 6B,D,F) indicate that in SARS-CoV-2-infected cells, positive loadings are strongly associated with tryptophan-related bands (e.g.,  $\sim 755$ , 1201, 1547, and  $1607\text{ cm}^{-1}$ ), along with lipid-associated C–H stretching modes ( $\sim 2850\text{--}2900\text{ cm}^{-1}$ ), reflecting altered amino-acid metabolism and membrane remodeling during infection. In contrast, MeV-infected cells show higher contributions from protein- and nucleic-acid-associated bands, including tyrosine- and guanine-related vibrations, particularly in the cytoplasm and Golgi-mitochondria regions. Using these intracellular Raman fingerprints, classification accuracies of 98.9% for SARS-CoV-2 and 97.2% for MeV were achieved, underscoring the potential of confocal

Raman microscopy for probing virus-host interactions and identifying COVID-19-related biomarkers. In another study, SERS-based aptasensor platform was developed for sensitive quantification of SARS-CoV-2 lysates.<sup>92</sup> The platform uses a spike protein DNA aptamer as a receptor and a self-grown Au nanopopcorn surface as the SERS detection substrate. By monitoring changes in the SERS peak intensity due to the binding between the aptamer DNA and the SARS-CoV-2 spike protein, the system enables detection with a LOD below 10 PFU/mL in under 15 min. This method shows significant potential for clinical application, offering improved detection limits and accuracy over current commercial SARS-CoV-2 immunodiagnostic kits.

The sensor system is fabricated using nanoimprint lithography and transfer printing, enabling large-area production on rigid and flexible substrates.<sup>49</sup> The study shows that the sensors, enhanced with metal–insulator–metal nanostructures, can detect viral samples, including spiked saliva, with a testing time of about 25 min and a detection accuracy of at least 83%. These techniques allow the sensors to distinguish between

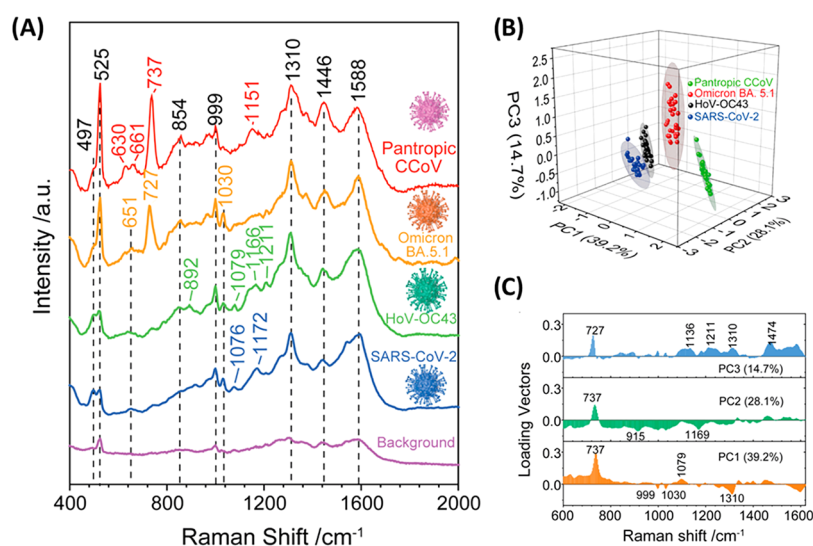


**Figure 7.** (A) Representative SERS spectra of SARS-CoV-2, human coronavirus OC43 (HCoV-OC43), SARS-CoV-2 Omicron variant BA.5.1, and CCoV, acquired on AuNP films under 785 nm excitation. Major diagnostic bands are labeled, and the background trace corresponds to virus-free control samples. (B) Three-dimensional PCA score plot showing clear clustering and separation of the four coronavirus types based on their SERS spectral signatures. (C) Corresponding PCA loading vectors for PC1, PC2, and PC3, highlighting the Raman bands contributing most strongly to virus discrimination. (Zhou, L.; Vestri, A.; Marchesano, V.; Rippa, M.; Sagnelli, D.; Picazio, G.; Fusco, G.; Han, J.; Zhou, J.; Petti, L. *The Label-Free Detection and Identification of SARS-CoV-2 Using Surface-Enhanced Raman Spectroscopy and Principal Component Analysis. Biosensors (Basel)* 2023, 13 (12). DOI: 10.3390/bios13121014) Adapted from ref 104.

different viral strains, including SARS-CoV-2 and other RNA viruses, with an accuracy ranging from 83 to 95%. Additionally, when viruses are grouped based on shared characteristics, such as respiratory versus nonrespiratory viruses, the classification accuracy improves. The platform also performs effectively in saliva-based testing, achieving 85–87% classification accuracy, suggesting that it could be used for noninvasive diagnostics. Another study developed a SERS platform based on MXene materials ( $\text{Nb}_2\text{C}$  and  $\text{Ta}_2\text{C}$ ) for detecting the SARS-CoV-2 spike protein.<sup>98</sup> Exploiting synergistic charge-transfer resonance and electromagnetic enhancement, the system achieved enhancement factors of  $3.0 \times 10^6$  ( $\text{Nb}_2\text{C}$ ) and  $1.4 \times 10^6$  ( $\text{Ta}_2\text{C}$ ) under 532 nm excitation.<sup>98</sup>  $\text{Ta}_2\text{C}$  demonstrated a detection limit of  $5 \times 10^{-9}$  M, enabling highly sensitive, real-time monitoring of viral proteins. This work highlights the potential of semiconductor-based MXenes in advancing rapid SERS diagnostics for SARS-CoV-2 and other viruses. A SERS platform using gold–copper nanostars enabled detection and characterization of SARS-CoV-2 virions along with their spike (S) and nucleocapsid (N) proteins.<sup>99</sup> Ethanol-inactivated virions and purified proteins produced consistent Raman fingerprints, with at least 15 virion-specific peaks overlapping with S and N. The method sensitively revealed structural features and conformational differences despite inactivation effects, offering a fast, label-free approach for viral detection and real-time protein monitoring. One recent study reported SERS-based aptasensor for ultrasensitive in situ detection of SARS-CoV-2 on solid surfaces.<sup>100</sup> Exploiting the multivalent presentation of spike proteins, Au@AgNPs self-assembled via aptamer binding to generate plasmonic hotspots, enabling detection within 20 min at a limit of 5.26 TCID<sub>50</sub>/mL. The sensor achieved 100% sensitivity and accuracy in blind testing of 20 contaminated packaging samples and outperformed ELISA across diverse materials. This approach demonstrates strong potential for real-world applications in cold-chain logistics, environmental surveillance, and public health monitoring. A microfluidic SERS platform was developed

to diagnose COVID-19 by trapping viruses from saliva, tears, and nasopharyngeal swabs and analyzing their spectral signatures.<sup>101</sup> Signal amplification was achieved using AuNP- and AgNP-coated carbon nanotubes within the device, enabling sensitive detection.

Another study demonstrates the detection of live SARS-CoV-2 S pseudovirus using gold nanocavities (AuNC) and gold nanoparticles on porous  $\text{ZrO}_2$  (AuNPs/p $\text{ZrO}_2$ ) to differentiate of the SARS-CoV-2 S pseudovirus from VSV-G pseudovirus by their characteristic Raman peaks.<sup>102</sup> The same group also presents a label-free SERS method for detecting and differentiating live SARS-CoV-2 variants, including A.3,  $\alpha$ , and Delta, based on their spike glycoprotein signatures.<sup>103</sup> Utilizing two custom SERS-active substrates, NCs and AuNPs/p $\text{ZrO}_2$ , the study demonstrated that variant-specific Raman peaks could be consistently detected at concentrations as low as  $10^3$ – $10^5$  copies/mL without preprocessing. The unique hotspot geometries of the substrates influenced peak profiles, enabling differentiation of variants through variations in specific spectral regions (e.g., 1208, 1400, and 1617  $\text{cm}^{-1}$ ). Notably, key peaks remained detectable even in the presence of interfering substances, confirming the method's robustness. Another study used an AuNP monolayer fabricated via liquid–liquid interfacial self-assembly to discriminate among several coronaviruses, including SARS-CoV-2, its Omicron BA.5.1 variant, human coronavirus OC43 (HCoV-OC43), and pantropic canine coronavirus (CCoV), using SERS combined with chemometric analysis.<sup>104</sup> As shown in Figure 7A, each virus exhibits distinct SERS fingerprints with characteristic Raman bands (see Table 4), while multivariate analysis enables clear clustering and separation of closely related coronavirus species and variants. In particular, the PCA score plot in Figure 7B demonstrates reliable discrimination between SARS-CoV-2 and the Omicron BA.5.1 variant, highlighting the capability of SERS-based chemometrics to resolve subtle biochemical differences associated with viral mutation. Detection limits below 100

TCID<sub>50</sub>/mL further underscore the sensitivity of this approach, supporting its potential for variant-aware coronavirus diagnostics. Further insight into the spectral origin of this separation is provided by the PCA loading vectors (Figure 7C), which identify the Raman bands contributing most strongly to virus discrimination. SARS-CoV-2 spectra cluster in the negative region of the first three principal components, with prominent contributions from bands near 915, 999, 1030, 1169, and 1310 cm<sup>-1</sup>. In contrast, HCoV-OC43 shares contributions from bands around 999, 1030, and 1310 cm<sup>-1</sup> but occupies distinct regions of PCA space, while the Omicron BA.5.1 variant and pantropic CCoV are differentiated by characteristic low-wavenumber features near 727 and 737 cm<sup>-1</sup>, respectively. Collectively, these results demonstrate that SERS combined with PCA can resolve subtle biochemical differences between closely related coronaviruses and variants. Because Raman spectroscopy probes phenotypic biochemical composition rather than specific genomic sequences, such approaches can remain informative even in the presence of sequence-level mutations. This highlights Raman spectroscopy as a complementary platform to genomics, particularly for variant screening, phenotypic strain clustering, and functional characterization.

Another study used SERS platform to detect and characterize structural proteins in SARS-CoV-2 and HIV-based virus-like particles (VLPs).<sup>105</sup> Using AuNPs aggregated with copper(II) sulfate (CuSO<sub>4</sub>), the study captured distinct SERS spectra that reflected the presence of spike (S) proteins, notably through intensity ratios at 842 and 858 cm<sup>-1</sup>. By applying machine learning (SVM, kNN, RF), they achieved classification accuracies up to 87.5% for SARS-CoV-2 VLPs and 92.5% for HIV-based VLPs. Raman spectroscopy and computational analysis, called Rametrix (Raman Chemometric Urinalysis), were developed to detect COVID-19 in urine that reflects systemic immune and metabolic responses.<sup>106</sup> The results were demonstrated 97.6% accuracy, 90.9% sensitivity, and 98.8% specificity when tested on urine samples from COVID-19 patients and control groups. Raman spectra of bead-virus complexes were analyzed with 1D correlation methods, enabling differentiation of SARS-CoV-2 from Influenza A and controls, with statistical validation by Kolmogorov–Smirnov testing.<sup>107</sup>

Raman spectroscopy, combined with machine learning, can also be applied to environmental samples. In this context, creating an angiotensin-converting enzyme 2 (ACE2)-functionalized gold nanoneedle “virus-trap” structure demonstrated the ability to detect a single virus. This system captured SARS-CoV-2 particles from contaminated water and enabled SERS detection to 80 copies/mL within 5 min using a 785 nm laser.<sup>88</sup> In another study, a rapid and on-site detection assay for SARS-CoV-2 in environmental water samples using SERS combined with ACE2-functionalized silver nanorods.<sup>108</sup> This novel “capture-quenching” system exploits the specific binding of the virus’s spike protein to ACE2, resulting in distinctive spectral shifts, particularly a red-shift from 1189 to 1182 cm<sup>-1</sup>. The assay allows ultrafast (within 5 min), RNA-extraction-free interrogation of viral presence in complex water matrices. On-site validation using portable Raman spectrometers across 23 water samples in Wuhan showed high accuracy (up to 93%) and strong agreement with RT-qPCR results. This method offers potential for wastewater-based epidemiology, environmental monitoring, and rapid viral detection in public health.

**MERS-CoV.** In a recent study, SERS using nanostructured Au substrates enabled sensitive detection of MERS in both synthetic particles and clinical samples.<sup>109</sup> Samples were dried

on the substrates and analyzed with a 785 nm laser (10 mW, 10 s acquisition), achieving a detection limit of 10<sup>2</sup> particles/mL. Calibration curves confirmed a direct correlation between Raman intensity and viral concentration, while clinical tests accurately distinguished infected from noninfected samples. The method showed high reproducibility across multiple days and substrate batches, underscoring its potential for viral diagnostics.

**SARS-CoV.** The study demonstrated that deep learning models can classify spike proteins from five coronaviruses, SARS-CoV-2, SARS-CoV, MERS-CoV, HCoV-OC43, and HCoV-229E, using Raman spectroscopy.<sup>110</sup> A total of 500 in vitro samples were analyzed using a 50 mW laser, and a neural network trained on the spectra achieved an accuracy of over 97%. The results matched experimental data, confirming distinct spectral differences and highlighting the potential of this approach for rapid, reliable coronavirus identification.

### Paramyxoviridae Family

**Nipah Virus (NiV).** The study utilized confocal micro-Raman spectroscopy to investigate receptor-induced conformational changes in the NiV glycoprotein (G) fusion (F), and glycoprotein (G), essential for viral entry and membrane fusion.<sup>111</sup> In this study, NiV VLPs were prepared by transfecting 293T cells with plasmids for NiV M, F, and G. Using a WITec alpha300 microscope with a 532.5 nm laser, the spectra were collected from viral samples on Au-coated slides. PCA differentiated the proteins M, F, and G spectral features. Additionally, to assess conformational changes, temperature and receptor-induced variations were analyzed. A NiV-G mutant was also used to confirm that the observed changes were specifically receptor-induced. The analysis was further validated by measuring the binding of a biotinylated HR2 peptide to the F protein. Additionally, 2D correlation Raman spectroscopy was employed for detailed spectral analysis. The method enabled real-time monitoring of conformational changes as the F and G proteins responded to temperature changes and receptor binding. Controls with the NiV-G mutant ensured distinction between temperature- and receptor-induced effects.

**Phenuiviridae Family. Rift Valley Fever Virus.** A SERS-based immunoassay was developed for multiplex detection of West Nile virus (WNV), Rift Valley fever virus (RVFV), and *Yersinia pestis* in serum using 60 nm AuNPs and ~200 nm Fe<sub>3</sub>O<sub>4</sub> magnetic nanoparticles.<sup>112</sup> Silica-encapsulated SERS nanotags conjugated with pathogen-specific antibodies enabled antigen capture, magnetic separation, and analysis with a portable Raman spectrometer. The assay achieved a detection limit of 10 pg/mL in fetal bovine serum and demonstrated high sensitivity and specificity for simultaneous virus detection. Silica encapsulation prevented cross-talk and preserved signal intensity, supporting accurate multiplexing and highlighting potential for real-time, on-site epidemic monitoring. Another study explores a magnetic capture-based SERS assay to detect virus-derived DNA sequences using Au-coated paramagnetic nanoparticles (Au@PMPs).<sup>113</sup> The developed assay detects target DNA sequences from the genomes of WNV and RVFV with high sensitivity. Au@PMPs serve as both the SERS substrate and a bioseparation reagent to capture target DNA, using complementary capture probes conjugated to Au@PMPs. Raman dyes, malachite green, and erythrosin B, conjugated to reporter probes specific to each target, provide distinct spectral signals. The assay protocol involves hybridizing target DNA with capture and reporter probes, followed by magnetic pull-down to concentrate the target DNA within the laser’s focus. The assay

distinguishes the individual and combined detection of WNV and RVFV DNAs through specific Raman peaks for each dye. Another study by the same group reporter-coated AuNPs and paramagnetic nanoparticles linked to specific antibodies, with 785 nm laser excitation of the complexes.<sup>114</sup> WNV and RVFV are distinguished through SERS amplification of their characteristic Raman spectra, Infrared 792 (IR-792) and Nile Blue. The assay yields detection limits of about 5 fg/mL in PBS and 25 pg/mL in PBS with fetal bovine serum.

For convenience, the most frequently reported Raman band assignments relevant to virion components and host-response signatures across the studies discussed above are summarized in Table 4.

## ■ CHALLENGES AND FUTURE DIRECTIONS

This section highlights key technical and biosafety constraints, along with practical mitigation strategies, while implications and perspectives across virus families are addressed in the Discussion section.

### Technical Challenges in Raman Spectroscopy for Virology

This section provides a brief overview of several intrinsic and technical constraints that limit the wider application of Raman spectroscopy in pandemic virology, together with representative mitigation strategies (Table 5) that have recently been

**Table 5. Mitigation Strategies for Fluorescence, Weak Raman Signals, and Spectral Complexity**<sup>11,24,29,30,48,73,79,80,88,91,109,126</sup>

challenge	strategy	mechanism
Autofluorescence/background	Near-IR excitation	Reduces fluorophore excitation
Weak Raman signal	SERS assays (LFA/microdevices)	Plasmonic field enhancement
Low capture/poor repeatability	Affinity capture (“virus-trap” etc.)	Target enrichment at hotspots
Spectral congestion/variability	Preprocessing, chemometrics	Baseline removal, variance separation
Subtle class separation	ML/deep learning	Nonlinear spectral pattern learning
Fluorescence-dominated imaging	Coherent Raman (CARS/SRS)	Fast nonlinear contrast; low fluorescence
Biosafety limits	Surrogates (inactivated/VLP/pseudotype)	Lower-BSL method development

demonstrated in virological and clinical studies. (i) One fundamental limitation is low signal intensity, as Raman scattering is inherently weak, typically, only 1 in 10 million photons contributes to a measurable signal.<sup>115</sup> This low efficiency necessitates either longer acquisition times or enhancement techniques, such as SERS or TERS, to achieve reliable detection, especially at low viral concentrations. (ii) Fluorescence interference is another critical issue. Biological samples, especially those containing pigments or aromatic compounds, often exhibit autofluorescence that can mask weak Raman signals. Techniques, such as CARS or shifting the excitation wavelength to the near-infrared range, are often employed to mitigate this problem; however, these add complexity to the experimental setup.<sup>116</sup> In practice, near-infrared excitation (e.g., 785–830 nm) has been successfully applied for WNV and RVFV antigen screening,<sup>114</sup> while coherent Raman modalities offer fluorescence-free contrast for rapid biochemical imaging of infected systems. (iii) Limited depth penetration also restricts Raman’s applicability for

studying virus-host interactions in thick tissues or 3D culture models. The technique is primarily surface-sensitive, making it better suited for single-cell or thin-layer analyses unless integrated with complementary imaging modalities.<sup>117</sup> (iv) Sample preparation also presents a significant challenge. Water, lipids, and proteins can interfere with Raman signal acquisition in biological matrices such as blood, saliva, or serum. (v) Another concern is that, isolating virus-specific signals without chemically altering the target analyte remains a critical hurdle. Standardizing sample handling protocols and integrating microfluidic<sup>101</sup> or filtration-based purification systems may help reduce biological noise and improve spectral reproducibility. Recent studies have demonstrated that affinity-based capture strategies, including aptamer-<sup>43,84</sup> or receptor-functionalized “virus-trap”<sup>88</sup> nanostructures, can selectively enrich intact virions at plasmonic hotspots, significantly improving signal reproducibility without chemical labeling. (vi) Spectral specificity is another concern. Raman signals can vary due to minor molecular changes or structural impurities, making it difficult to distinguish closely related viruses or viral subtypes. This limitation is increasingly addressed through multivariate chemometrics<sup>57</sup> and machine-learning approaches,<sup>78,119,120</sup> which can extract subtle, nonobvious spectral features and have enabled robust discrimination between closely related respiratory viruses in complex clinical data sets. (vii) Additionally, standardization across Raman platforms remains inadequate, affecting reproducibility across laboratories. Developing centralized, open-access Raman databases and implementing interlaboratory calibration protocols could help address reproducibility issues and facilitate broader clinical adoption. (viii) Lastly, the cost and accessibility of advanced Raman systems, such as TERS or confocal Raman microscopes, present practical barriers for widespread adoption due to significant capital investment and trained personnel for operation and data interpretation.<sup>115,118</sup>

Despite these limitations, Raman spectroscopy continues to evolve rapidly as researchers address them, as seen in Table 5. Innovations in nanomaterials, AI-driven spectral analysis, and portable instrumentation are likely to overcome many of these challenges, establishing Raman-based platforms as essential tools in virological research and diagnostics. To support future clinical use, greater focus should be on miniaturizing Raman instruments, integrating user-friendly software workflows, and developing reliable, automated data interpretation pipelines. Portable or hand-held Raman devices,<sup>84</sup> equipped with fiber-optic probes or microfluidic interfaces,<sup>101</sup> are particularly valuable for point-of-care applications, enabling rapid viral screening directly at triage points, clinics, or field stations. However, successful implementation will require reinforced hardware capable of operating under variable environmental conditions (e.g., humidity, temperature fluctuations), battery-powered system for off-grid use, and simplified calibration protocols that eliminate the need for expert alignment. On the software side, real-time preprocessing algorithms, which are capable of noise reduction, baseline correction, and peak normalization, must be integrated with AI-driven classification models to provide on-the-spot diagnostic readouts with minimal user input. RAMANMETRIX<sup>119,120</sup> is an example of software that integrates all these features for Raman spectroscopic data in biochemical samples, showing high potential for clinical applications.<sup>119</sup> Additionally, interoperability with electronic medical records and mobile health platforms would allow seamless data transfer and epidemiological tracking.<sup>121</sup> Collectively, these technical advancements help to transform

Raman spectroscopy from a laboratory research tool into a frontline diagnostic solution during outbreaks and in resource-constrained settings.

In addition to technical considerations, the clinical translation of Raman spectroscopy is also significantly impacted by regulatory hurdles. Raman-based systems intended for diagnostic or clinical use must comply with strict medical device regulations, including those established by the U.S. Food and Drug Administration (FDA), the European Medicines Agency (EMA), and regional regulatory authorities. For instance, under the FDA framework, Raman systems must typically undergo 510(k) clearance or De Novo classification, requiring substantial clinical validation, risk assessments, and demonstration of analytical performance, steps that are both time-consuming and resource-intensive.<sup>122</sup> Similarly, the European Union's Medical Device Regulation (MDR 2017/745) enforces strict guidelines for conformity assessment, clinical evaluation, and postmarket surveillance. These frameworks demand robust clinical trial data and device-specific quality management systems (e.g., ISO 13485 compliance), which often exceed the scope of academic or exploratory research settings.<sup>123</sup> Moreover, the use of AI and machine learning algorithms in Raman diagnostics introduces further complexity, as these fall under Software as a Medical Device classifications.<sup>124</sup> Regulatory authorities now require explainability, traceability, and real-time performance monitoring of these AI tools, criteria that many current Raman-AI studies do not yet meet. This evolving regulatory landscape, while necessary for ensuring patient safety, contributes to delays in translating even validated Raman technologies into deployable clinical solutions.<sup>125</sup> Bridging this gap will require early stage collaboration with regulatory experts, inclusion of validation cohorts in initial study designs, and adherence to clinical-grade development standards throughout the pipeline. Regulatory science literacy must become an integral part of translational Raman research to facilitate timely approval and global accessibility.

### Virological and Biosafety Challenges in Pandemic Virus Research

Due to biosafety concerns, Raman spectroscopy applications have mainly focused on nonpandemic viruses.<sup>141</sup> Research on pandemic viruses faces major challenges involving biosafety, technical limitations, and ethics. Handling agents such as SARS-CoV-2, H1N1, or Ebola requires BSL-3 or BSL-4 laboratories with advanced filtration, waste control, and strict entry systems. These facilities add complexity and limit access to trained personnel. Full protective gear further reduces dexterity, hampers communication, and increases fatigue. Any accidental exposure poses serious health risks, demanding strict compliance with safety standards.<sup>126</sup> In vitro work offers control but selecting suitable cell lines, as not all replicate human infections accurately. Viral mutations during experiments can also complicate results.<sup>127,128</sup> In vivo studies face similar issues in identifying animal models that mirror human disease. Many species show different infection dynamics and immune responses. Ethical concerns are greater with higher-order animals and require strong oversight. Individual variability and transmission risks among animals add further complications.<sup>129</sup> Ex vivo models using isolated tissues provide a middle ground but face limits in maintaining viability and reproducing immune or circulatory conditions. Access to fresh tissues can also be difficult during outbreaks.<sup>128</sup> Studies using human samples require strict informed consent, privacy protection, and

biobanking policies.<sup>130</sup> International collaborations often add regulatory complexity due to differing ethical standards.<sup>131,132</sup> Another critical issue is "gain-of-function" research, enhancing viral spread or virulence, which remains controversial and tightly regulated.<sup>133</sup> Ethical safeguards, risk-benefit analysis, community input, and independent review are essential. Public trust depends on transparency, as misinformation about biosafety can undermine support for legitimate research.<sup>133</sup> Data interpretation in pandemic studies is complicated by strain variability, cross-species differences, and reproducibility issues. Rapid viral evolution makes generalization difficult.<sup>134</sup> Animal data often fail to translate directly to humans, and small procedural differences in high-containment work can alter results.<sup>134,135</sup>

Beyond the shared biosafety, technical, and ethical challenges that complicate pandemic virus research, a clear trend emerges in the Raman spectroscopy literature. Certain viruses, particularly Influenza and SARS-CoV-2, appear far more frequently in experimental studies than others such as Marburg, Lassa, or Ebola. While this imbalance partly reflects biosafety-level constraints, since viruses requiring BSL-3 laboratories like SARS-CoV-2 and H1N1 are more accessible than BSL-4 viruses, it is also influenced by additional factors. Viruses with higher transmissibility and replication rates, not only present a greater public health threat but also necessitate constant monitoring and diagnostic innovation,<sup>136</sup> making them attractive targets for rapid, label-free analytical tools like Raman spectroscopy.<sup>137–138,139,140</sup>

Moreover, viruses with high mutation rates, such as Influenza<sup>41,44</sup> and SARS-CoV-2,<sup>104</sup> present ongoing challenges for target-specific diagnostics, motivating interest in complementary phenotypic detection strategies. Unlike assays that rely on predefined molecular targets and may lose sensitivity due to sequence drift, Raman spectroscopy interrogates the global biochemical phenotype of virions and infected systems, including proteins,<sup>84</sup> lipids, glycosylation patterns, and RNA packing.<sup>41,44,104,144</sup> As demonstrated for coronaviruses and their variants (Figure 7), Raman-based signatures can remain informative despite antigenic variation, enabling chemometric or AI-assisted clustering of closely related strains based on surface chemistry<sup>43</sup> and host-response features. Accordingly, Raman spectroscopy should be viewed as complementary to genomic approaches. While the sequencing provides viral mutation profiles, Raman methods provide functional and structural phenotypic information that reflects viral composition and infection state, supporting variant screening and phenotypic characterization rather than replacing molecular diagnostics.<sup>144</sup>

Research on pandemic viruses is further accelerated by the widespread availability of viral strains, pseudoviruses, reagents, and commercial kits, often distributed through global biorepositories. Large-scale international collaborations and pandemic-era funding mechanisms have also concentrated resources on these pathogens, enhancing both data sharing and technological innovation. Finally, public health priorities and political attention significantly affect research direction in that viruses perceived as urgent due to global spread or zoonotic potential attract more funding and visibility. In contrast, equally dangerous but regionally contained viruses like Ebola and CCHF, despite their high mortality, remain underrepresented due to limited access, fewer resources, and lower integration into global surveillance infrastructures. Taken together, these interlinked biological, logistical, and sociopolitical factors explain why Raman spectroscopy has been applied more extensively to certain pandemic viruses than to others.

Importantly, the limited detection of high-risk viruses by Raman spectroscopy does not hinder meaningful research, since several safe and validated methods are available. Although studies involving live MARV, EBOV, LASV, and CCHFV require BSL-4 facilities, Raman spectroscopy can still be effectively performed using safer surrogate systems. These include (i) chemically<sup>99</sup> or thermally<sup>87</sup> inactivated virions that retain surface glycoprotein; (ii) UV-inactivated stocks optimized to preserve protein secondary structure;<sup>147</sup> (iii) recombinant envelope or nucleocapsid proteins<sup>89,94</sup> for band assignment and sensor calibration; (iv) VLPs that reproduce native membrane/capsid composition without genomes;<sup>105,111</sup> and (v) pseudotyped viruses expressing the relevant entry proteins on lower-risk backbones. Such systems can be handled at BSL-2/3, enabling spectral library building, substrate optimization, and AI-training data sets before validation with authentic pathogens. These approaches are particularly well suited to Raman-based studies, as they preserve key molecular and surface features relevant to spectral fingerprinting while enabling systematic method development and machine-learning model training under accessible biosafety conditions.

## DISCUSSION

Building on the challenges and solutions discussed in the [Challenges and Future Directions](#) section, this discussion section synthesizes virus-dependent trends, translational readiness, and future research priorities, rather than repeating methodological limitations. The use of Raman spectroscopy in virology has gained significant momentum recently, especially for molecular-level analysis and rapid diagnostics. However, its practical application still remains limited to some viruses. This review highlights the progress made over the years and current gaps in pandemic virology using Raman spectroscopy. Not only technical limitations but also virus-dependent limitations are also taken into account in detail. For instance, Influenza studies have utilized SERS for subtype identification, antiviral resistance detection,<sup>47</sup> and virulence profiling,<sup>44</sup> while SARS-CoV-2 research spans from virus identification in clinical fluids (e.g., saliva, serum, nasopharyngeal swabs),<sup>75–80</sup> even in environmental samples<sup>88</sup> to machine learning-enhanced diagnostics and point-of-care sensor development.<sup>36,48,79</sup> These examples demonstrate the versatility and sensitivity of Raman-based techniques, especially when paired with plasmonic substrates and advanced data analysis. By contrast, several pandemic-prone virus families, including Filoviridae (Marburg, Ebola), Arenaviridae (Lassa), and Nairoviridae (CCHF), are still largely unexplored in Raman research. Based on these findings, Raman virology research mainly focuses on viruses that have a significant global impact, are safe to handle at accessible biosafety levels, spread efficiently, and mutate often. Influenza A subtypes and SARS-CoV-2 have attracted the most attention, reflecting both their pandemic relevance and the availability of clinical or laboratory samples. All these data sets research ranging from biochemical fingerprinting to clinically relevant diagnostics. For example, SERS-based investigations on SARS-CoV-2 have demonstrated high sensitivity with nasopharyngeal swabs;<sup>78,79</sup> however, translation into clinical tests is still limited by substrate reproducibility and sample variability. Similarly, influenza studies have revealed replication dynamics at the single-cell level,<sup>25,41</sup> but remain largely limited to laboratory settings rather than clinical validation. By contrast, viruses such as Ebola, Marburg, and Lassa are underrepresented, not because of lesser importance, but due to the lack of Raman studies on

BSL-4 viruses. However, this does not fully explain the gap in certain viruses research. Evidence from SARS-CoV-2 and dengue shows that Raman methods can be applied to inactivated viruses, pseudovirions, or recombinant proteins under standard laboratory conditions. The shortage of Raman data likely stems from practical challenges rather than scientific limitations. Restricted access to reagents, low research prioritization, funding limitations, and the lack of curated spectral libraries all contribute to this gap. Poliovirus is a striking example: despite its historic impact and the availability of vaccines, no Raman studies have been performed on the live virus itself, with work focusing only on vaccine formulations.<sup>66</sup> Beyond these technical gaps, progress toward clinical translation has been inconsistent. SARS-CoV-2 and influenza assays already show strong sensitivity for viral load<sup>36</sup> and subtype detection<sup>43</sup> in patient samples, highlighting their diagnostic promise. Portable SERS devices<sup>84</sup> and saliva-based Raman tests<sup>80</sup> further demonstrate that point-of-care use is possible. However, most of these approaches remain at the proof-of-concept stage and will need rigorous validation in clinical trials before they can be widely adopted.

Despite recent progress, limited penetration depth<sup>117</sup> hinders applications in tissues and organoids. Among Raman modalities, SERS has clearly become the preferred choice, valued for its sensitivity and compatibility with portable diagnostic platforms. Studies have confirmed its ability to detect viruses even at very low concentrations and in challenging settings. During the COVID-19 pandemic, its capability proved useful for detecting viruses. Some studies have utilized confocal Raman imaging to track virus-induced biochemical changes, such as altered protein folding or amino acid profiles, inside host cells.<sup>53,58,63,71,97</sup> For instance, SARS-CoV-2 infection has been linked to increased tryptophan levels<sup>97</sup> and distinct molecular signatures compared to other RNA viruses. Similarly, several dengue virus studies have detected disease-specific markers like ADP<sup>53</sup> and soluble ST2<sup>58</sup> in serum, while Zika<sup>63</sup> and monkeypox virus<sup>71</sup> studies leveraged SERS-based assays to distinguish closely related viruses through subtle spectral shifts. These findings underscore the ability of Raman spectroscopy not only to identify viruses but also to capture pathophysiological responses in the host. This makes it a dual-purpose platform for diagnostics and mechanistic understanding. However, although AI-driven SERS approaches have advanced viral diagnostics, fundamental studies of viral mechanisms remain limited. High-resolution Raman modalities, including TERS, CARS, and SRS, offer powerful tools for probing viral structure, surface chemistry, and virus-host interactions at the nanoscale. Broader and systematic application of these approaches is expected to expand virus coverage, diversify Raman-based virological applications, and enhance diagnostic and surveillance preparedness for emerging viral threats. At present, CARS should be regarded as promising future extensions of nanoscale viral spectroscopy rather than established virus-identification platforms, pending direct experimental validation on intact virions.<sup>25,148</sup>

Machine learning has become indispensable for Raman-based virology because spectra from clinical matrices are high-dimensional and subject to interpatient and interinstrument variability. Typical pipelines include (i) preprocessing<sup>86</sup> (cosmic-ray removal, smoothing, baseline correction, and normalization), (ii) dimensionality reduction,<sup>40,56</sup> and (iii) supervised classification (SVM,<sup>46</sup> Random Forest,<sup>49</sup> kNN,<sup>105</sup> PLS-DA<sup>82</sup>). In pandemic-relevant studies, AI has enabled reliable separation of closely related respiratory viruses and

discrimination between positive and negative clinical samples, even at low viral loads.<sup>36</sup> Importantly, model explainability approaches are beginning to link predictive Raman bands to biochemical mechanisms in broader biomedical Raman applications.<sup>29,97,144</sup> Future progress relies on multicenter spectral libraries, standardized preprocessing, and ongoing model updates for new variants and population differences.

Besides biofluid and swab diagnostics, Raman spectroscopy could enhance outbreak readiness through the detection of airborne viruses. Aerosolized virions can be captured with plasmonic fibrous filters, nanofluidic impactors, or electrostatic collectors that are integrated with SERS-active surfaces. These are then followed by rapid spectral readout and AI-assisted classification. Such systems could enable continuous monitoring in high-risk indoor environments, including healthcare facilities, transportation hubs, and animal housing units, and would complement established wastewater-based epidemiology approaches. Integration of autonomous sampling hardware with real-time Raman-AI pipelines could ultimately support early warning surveillance networks for emerging respiratory pathogens.<sup>150</sup>

## CONCLUSIONS

This review provides a comprehensive and focused synthesis of the applications of Raman spectroscopy in studying pandemic and high-consequence viruses. It highlights the unique potential of Raman spectroscopy as a label-free, noninvasive tool for investigating viral structure, host–virus interactions, and infection-related biochemical changes. Studies on pandemic-relevant viruses, particularly influenza and SARS-CoV-2, demonstrate the value of Raman-based approaches for identifying viruses, profiling their phenotypes, and providing complementary diagnostics. However, this review also critically examines the technical, analytical, regulatory, and biosafety challenges that limit its broader adoption. These challenges include weak intrinsic signal intensity, fluorescence interference, limited depth penetration, sample complexity, spectral specificity, a lack of standardization, high system cost, and barriers to clinical translation. Looking forward, advances in nanostructured substrates, affinity-based enrichment strategies, coherent Raman modalities, AI-driven spectral analysis, and portable instrumentation are expected to address many of these limitations. The review emphasizes that the limited application of Raman spectroscopy to several high-consequence viruses is due to biosafety constraints, strategic gaps, and infrastructural limitations. These limitations can be mitigated by using inactivated virions, recombinant proteins, virus-like particles, and pseudotyped systems under lower biosafety conditions. Together, these developments position Raman spectroscopy as a complementary, increasingly translational technology in virology with significant potential to deepen molecular insight, improve diagnostic preparedness, and support equitable, global pandemic response efforts.

## AUTHOR INFORMATION

### Corresponding Author

**Jürgen Popp** – Member of Leibniz Health Technologies, Member of the Leibniz Centre for Photonics in Infection Research (LPI), Leibniz Institute of Photonic Technology, 07745 Jena, Germany; Member of the Leibniz Centre for Photonics in Infection Research (LPI), Institute of Physical Chemistry (IPC) and Abbe Center of Photonics (ACP),

Friedrich Schiller University Jena, 07743 Jena, Germany; InfectoGnostics Research Campus Jena, Center of Applied Research, Jena 07743, Germany; [orcid.org/0000-0003-4257-593X](https://orcid.org/0000-0003-4257-593X); Email: [juergen.popp@leibniz-ipht.de](mailto:juergen.popp@leibniz-ipht.de)

## Authors

**Hulya Yilmaz** – Member of Leibniz Health Technologies, Member of the Leibniz Centre for Photonics in Infection Research (LPI), Leibniz Institute of Photonic Technology, 07745 Jena, Germany; Member of the Leibniz Centre for Photonics in Infection Research (LPI), Institute of Physical Chemistry (IPC) and Abbe Center of Photonics (ACP), Friedrich Schiller University Jena, 07743 Jena, Germany; [orcid.org/0000-0003-4592-6432](https://orcid.org/0000-0003-4592-6432)

**Anuradha Ramoji** – Member of Leibniz Health Technologies, Member of the Leibniz Centre for Photonics in Infection Research (LPI), Leibniz Institute of Photonic Technology, 07745 Jena, Germany; Member of the Leibniz Centre for Photonics in Infection Research (LPI), Institute of Physical Chemistry (IPC) and Abbe Center of Photonics (ACP), Friedrich Schiller University Jena, 07743 Jena, Germany

**Andreea Winterfeld** – Member of Leibniz Health Technologies, Member of the Leibniz Centre for Photonics in Infection Research (LPI), Leibniz Institute of Photonic Technology, 07745 Jena, Germany

**Hamideh Salehi** – University of Strasbourg, ICube UMR 7357, CNRS, Inserm, Strasbourg 67000, France

**Aykut Ozkul** – Department of Virology, Faculty of Veterinary Medicine, Ankara University, Ankara 06070, Turkey

Complete contact information is available at:

<https://pubs.acs.org/10.1021/acsp Photonics.5c02174>

## Author Contributions

Conceptualization, H.Y.; writing-original draft preparation, H.Y.; writing-review and editing, H.Y., A.R., A.W., H.S., A.O., J.P.; supervision, A.R., A.O., J.P. The authors confirm that each author has contributed significantly to the preparation of this work and approved the final version for submission.

## Funding

This research was supported by the German Federal Ministry of Education and Research (BMBF) under the Photonic Research Germany funding program (projects “LPI-BT1-FSU,” FKZ 13N15466; “LPI-BT2-IPHT,” FKZ 13N15704; and “SARS-CoV-2Dx,” FKZ: 13N15745). The work is integrated into the Leibniz Center for Photonics in Infection Research (LPI), which is part of the BMBF national roadmap for research infrastructures.

## Notes

The authors declare no competing financial interest.

## ACKNOWLEDGMENTS

The authors acknowledge Dr. Cavit Agca for assistance with reference formatting.

## REFERENCES

- (1) Neumann, G.; Kawaoka, Y. Which Virus Will Cause the Next Pandemic? *Viruses* **2023**, *15* (1), 199.
- (2) Ramoji, A.; Pahlow, S.; Pistiki, A.; Rueger, J.; Shaik, T. A.; Shen, H.; Wichmann, C.; Krafft, C.; Popp, J. Understanding viruses and viral infections by biophotonic methods. *Translational Biophotonics* **2022**, *4* (1–2), e202100008 DOI: [10.1002/tbio.202100008](https://doi.org/10.1002/tbio.202100008).

- (3) Liu, D.; Pan, L.; Zhai, H.; Qiu, H. J.; Sun, Y. Virus tracking technologies and their applications in viral life cycle: research advances and future perspectives. *Front. Immunol.* **2023**, *14*, No. 1204730.
- (4) Maginnis, M. S. Virus-Receptor Interactions: The Key to Cellular Invasion. *J. Mol. Biol.* **2018**, *430* (17), 2590–2611.
- (5) Jones, J. E.; Le Sage, V.; Lakdawala, S. S. Viral and host heterogeneity and their effects on the viral life cycle. *Nat. Rev. Microbiol.* **2021**, *19* (4), 272–282.
- (6) Idrees, S.; Chen, H.; Panth, N.; Paudel, K. R.; Hansbro, P. M. Exploring Viral-Host Protein Interactions as Antiviral Therapies: A Computational Perspective. *Microorganisms* **2024**, *12* (3), 630.
- (7) Datta, S.; Hett, E. C.; Vora, K. A.; Hazuda, D. J.; Oslund, R. C.; Fadeyi, O. O.; Emili, A. The chemical biology of coronavirus host-cell interactions. *RSC Chem. Biol.* **2021**, *2* (1), 30–46.
- (8) Merenich, D. K. E. V. M.-B. C. J. K. A. M. Advanced microscopy techniques for the visualization and analysis of cell behaviors. In *Cell Movement in Health and Disease*; Michael Schnoor, L.-M. Y.; Sean, X. Sun., Eds.; Academic Press, 2022.
- (9) Kianzad, S.; SeyedAlinaghi, S.; Asadollahi-Amin, A.; Dadras, O.; Karimi, A.; Afsahi, A. M.; MohsseniPour, M.; Barzegary, A.; Mirzapour, P.; Mirghaderi, S. P. et al. Comparison of SARS-CoV-2 (Coronavirus) with other Similar Viruses Based on Current Evidence. *J. Iranian Med. Council* **2022** DOI: 10.18502/jimc.v5i1.9565.
- (10) Islam, M. T.; Quispe, C.; Herrera-Bravo, J.; Sarkar, C.; Sharma, R.; Garg, N.; Fredes, L. I.; Martorell, M.; Alshehri, M. M.; Sharifi-Rad, J.; et al. Production, Transmission, Pathogenesis, and Control of Dengue Virus: A Literature-Based Undivided Perspective. *Biomed. Res. Int.* **2021**, *2021*, No. 4224816.
- (11) Ruokola, P.; Dadu, E.; Kazmertsuk, A.; Hakkanen, H.; Marjomaki, V.; Ihalainen, J. A. Raman spectroscopic signatures of echovirus 1 uncoating. *J. Virol.* **2014**, *88* (15), 8504–8513.
- (12) Organization, W. H. WHO reports CDC, 2014 <https://www.bbc.com/news/world-africa-29769782>.
- (13) Goldsmith, C. S.; Miller, S. E. Modern uses of electron microscopy for detection of viruses. *Clin. Microbiol. Rev.* **2009**, *22* (4), 552–563.
- (14) Schaack, G. A.; Mehle, A. Experimental Approaches to Identify Host Factors Important for Influenza Virus. *Cold Spring Harb Perspect Med.* **2020**, *10* (12), a038521 DOI: 10.1101/cshperspect.a038521.
- (15) Jansz, N.; Faulkner, G. J. Viral genome sequencing methods: benefits and pitfalls of current approaches. *Biochem. Soc. Trans.* **2024**, *52* (3), 1431–1447.
- (16) Mahmud, I.; Garrett, T. J. Mass Spectrometry Techniques in Emerging Pathogens Studies: COVID-19 Perspectives. *J. Am. Soc. Mass Spectrom.* **2020**, *31* (10), 2013–2024.
- (17) Garg, T.; Weiss, C. R.; Sheth, R. A. Techniques for Profiling the Cellular Immune Response and Their Implications for Interventional Oncology. *Cancers* **2022**, *14* (15), 3628.
- (18) Oumarou Hama, H.; Aboudharam, G.; Barbieri, R.; Lepidi, H.; Drancourt, M. Immunohistochemical diagnosis of human infectious diseases: a review. *Diagn. Pathol.* **2022**, *17* (1), 17.
- (19) Iwanami, S.; Kitagawa, K.; Ohashi, H.; Asai, Y.; Shionoya, K.; Saso, W.; Nishioka, K.; Inaba, H.; Nakaoka, S.; Wakita, T.; et al. Should a viral genome stay in the host cell or leave? A quantitative dynamics study of how hepatitis C virus deals with this dilemma. *PLoS Biol.* **2020**, *18* (7), No. e3000562.
- (20) Ferrarini, M. G.; Lal, A.; Rebollo, R.; Gruber, A. J.; Guarracino, A.; Gonzalez, I. M.; Floyd, T.; de Oliveira, D. S.; Shanklin, J.; Beausoleil, E.; et al. Genome-wide bioinformatic analyses predict key host and viral factors in SARS-CoV-2 pathogenesis. *Commun. Biol.* **2021**, *4* (1), 590.
- (21) Ashmore-Harris, C.; Iafraite, M.; Saleem, A.; Fruhwirth, G. O. Non-invasive Reporter Gene Imaging of Cell Therapies, including T Cells and Stem Cells. *Mol. Ther.* **2020**, *28* (6), 1392–1416.
- (22) Jones, R. R.; Hooper, D. C.; Zhang, L.; Wolverson, D.; Valev, V. K. Raman Techniques: Fundamentals and Frontiers. *Nanoscale Res. Lett.* **2019**, *14* (1), 231.
- (23) Fernández-Galiana, Á.; Bibikova, O.; Vilms Pedersen, S.; Stevens, M. M. Fundamentals and Applications of Raman-Based Techniques for the Design and Development of Active Biomedical Materials. *Adv. Mater.* **2024**, *36* (43), No. e2210807.
- (24) Cialla-May, D.; Krafft, C.; Rosch, P.; Deckert-Gaudig, T.; Frosch, T.; Jahn, I. J.; Pahlow, S.; Stiebing, C.; Meyer-Zedler, T.; Bocklitz, T.; et al. Raman Spectroscopy and Imaging in Bioanalytics. *Anal. Chem.* **2022**, *94* (1), 86–119.
- (25) Deckert, V.; Deckert-Gaudig, T.; Cialla-May, D.; Popp, J.; Zell, R.; Deinhard-Emmer, S.; Sokolov, A. V.; Yi, Z.; Scully, M. O. Laser spectroscopic technique for direct identification of a single virus I: FASTER CARS. *Proc. Natl. Acad. Sci. U. S. A.* **2020**, *117* (45), 27820–27824.
- (26) Xu, D.; Liang, B.; Xu, Y.; Liu, M. Recent advances in tip-enhanced Raman spectroscopy probe designs. *Nano Res.* **2023**, *16* (4), 5555–5571.
- (27) Höppener, C.; Aizpurua, J.; Chen, H.; Gräfe, S.; Jorio, A.; Kupfer, S.; Zhang, Z.; Deckert, V. Tip-enhanced Raman scattering. *Nature Reviews Methods Primers* **2024**, *4* (1), 47 DOI: 10.1038/s43586-024-00323-5.
- (28) Tian, Z. Y. M.; VB; Zhang, X.; Khalil, M.; Ayejoto, D. A. Coherent Anti-Stokes Raman Scattering. In *Advanced Diagnostics in Combustion Science*; Springer, 2023.
- (29) Zhang, C.; Zhang, D.; Cheng, J. X. Coherent Raman Scattering Microscopy in Biology and Medicine. *Annu. Rev. Biomed Eng.* **2015**, *17*, 415–445.
- (30) Cheng, Q.; Miao, Y.; Wild, J.; Min, W.; Yang, Y. Emerging applications of stimulated Raman scattering microscopy in materials science. *Matter* **2021**, *4* (5), 1460–1483.
- (31) Orlando, A.; Franceschini, F.; Muscas, C.; Pidkova, S.; Bartoli, M.; Rovere, M.; Tagliaferro, A. A Comprehensive Review on Raman Spectroscopy Applications. *Chemosensors* **2021**, *9* (9), 262.
- (32) Lukose, J.; Barik, A. K.; Mithun, N.; Sanoop Pavithran, M.; George, S. D.; Murukeshan, V. M.; Chidangil, S. Raman spectroscopy for viral diagnostics. *Biophys Rev.* **2023**, *15* (2), 199–221.
- (33) Lisyansky, A. A. A.; E S; Vinogradov, A. P.; Shishkov, V. Y. Surface-Enhanced Raman Scattering. In: *Quantum Optics of Light Scattering, Springer Series in Optical Sciences*; Springer, 2024.
- (34) Kumar, N.; Mignuzzi, S.; Su, W.; Roy, D. Tip-enhanced Raman spectroscopy: principles and applications. *EPJ Techniques Instrumentation* **2015**, *2* (1), 9 DOI: 10.1140/epjti/s40485-015-0019-5.
- (35) Wang, X.; Li, S.; Qu, H.; Hao, L.; Shao, T.; Wang, K.; Xia, Z.; Li, Z.; Li, Q. SERS-based immunomagnetic bead for rapid detection of H5N1 influenza virus. *Influenza Other Respir. Viruses* **2023**, *17* (3), No. e13114.
- (36) Park, H. J.; Yang, S. C.; Choo, J. Early Diagnosis of Influenza Virus A Using Surface-enhanced Raman Scattering-based Lateral Flow Assay. *Bulletin Korean Chem. Society* **2016**, *37* (12), 2019–2024.
- (37) Xiao, M.; Xie, K.; Dong, X.; Wang, L.; Huang, C.; Xu, F.; Xiao, W.; Jin, M.; Huang, B.; Tang, Y. Ultrasensitive detection of avian influenza A (H7N9) virus using surface-enhanced Raman scattering-based lateral flow immunoassay strips. *Anal. Chim. Acta* **2019**, *1053*, 139–147.
- (38) Wang, C.; Wang, C.; Wang, X.; Wang, K.; Zhu, Y.; Rong, Z.; Wang, W.; Xiao, R.; Wang, S. Magnetic SERS Strip for Sensitive and Simultaneous Detection of Respiratory Viruses. *ACS Appl. Mater. Interfaces* **2019**, *11* (21), 19495–19505.
- (39) Zhang, D.; Huang, L.; Liu, B.; Ge, Q.; Dong, J.; Zhao, X. Rapid and Ultrasensitive Quantification of Multiplex Respiratory Tract Infection Pathogen via Lateral Flow Microarray based on SERS Nanotags. *Theranostics* **2019**, *9* (17), 4849–4859.
- (40) Lim, J. Y.; Nam, J. S.; Yang, S. E.; Shin, H.; Jang, Y. H.; Bae, G. U.; Kang, T.; Lim, K. I.; Choi, Y. Identification of Newly Emerging Influenza Viruses by Surface-Enhanced Raman Spectroscopy. *Anal. Chem.* **2015**, *87* (23), 11652–11659.
- (41) Dardir, K.; Wang, H.; Martin, B. E.; Atzampou, M.; Brooke, C. B.; Fabris, L. SERS Nanoprobe for Intracellular Monitoring of Viral Mutations. *J. Phys. Chem. C* **2020**, *124* (5), 3211–3217.
- (42) Sun, Y.; Xu, L.; Zhang, F.; Song, Z.; Hu, Y.; Ji, Y.; Shen, J.; Li, B.; Lu, H.; Yang, H. A promising magnetic SERS immunosensor for

sensitive detection of avian influenza virus. *Biosens. Bioelectron.* **2017**, *89* (Pt 2), 906–912.

(43) Kukushkin, V. I.; Ivanov, N. M.; Novoseltseva, A. A.; Gambaryan, A. S.; Yaminsky, I. V.; Kopylov, A. M.; Zavyalova, E. G. Highly sensitive detection of influenza virus with SERS aptasensor. *PLoS One* **2019**, *14* (4), No. e0216247.

(44) Negri, P.; Chen, G.; Kage, A.; Nitsche, A.; Naumann, D.; Xu, B.; Dluhy, R. A. Direct optical detection of viral nucleoprotein binding to an anti-influenza aptamer. *Anal. Chem.* **2012**, *84* (13), 5501–5508.

(45) Zhang, Z.; Jiang, S.; Wang, X.; Dong, T.; Wang, Y.; Li, D.; Gao, X.; Qu, Z.; Li, Y. A novel enhanced substrate for label-free detection of SARS-CoV-2 based on surface-enhanced Raman scattering. *Sens Actuators B Chem.* **2022**, *359*, No. 131568.

(46) Tabarov, A.; Vitkin, V.; Andreeva, O.; Shemanaeva, A.; Popov, E.; Dobroslavin, A.; Kurikova, V.; Kuznetsova, O.; Grigorenko, K.; Tzibizov, I.; et al. Detection of A and B Influenza Viruses by Surface-Enhanced Raman Scattering Spectroscopy and Machine Learning. *Biosensors* **2022**, *12* (12), 1065.

(47) Eom, G.; Hwang, A.; Kim, H.; Yang, S.; Lee, D. K.; Song, S.; Ha, K.; Jeong, J.; Jung, J.; Lim, E. K.; Kang, T. Diagnosis of Tamiflu-Resistant Influenza Virus in Human Nasal Fluid and Saliva Using Surface-Enhanced Raman Scattering. *ACS Sens* **2019**, *4* (9), 2282–2287.

(48) Chen, H.; Das, A.; Bi, L.; Choi, N.; Moon, J.-I.; Wu, Y.; Park, S.; Choo, J. Recent advances in surface-enhanced Raman scattering-based microdevices for point-of-care diagnosis of viruses and bacteria. *Nanoscale* **2020**, *12* (42), 21560–21570.

(49) Paria, D.; Kwok, K. S.; Raj, P.; Zheng, P.; Gracias, D. H.; Barman, I. Label-Free Spectroscopic SARS-CoV-2 Detection on Versatile Nanoimprinted Substrates. *Nano Lett.* **2022**, *22* (9), 3620–3627.

(50) Sebba, D.; Lastovich, A. G.; Kuroda, M.; Fallows, E.; Johnson, J.; Ahouidi, A. N.; Honko, A. N.; Fu, H.; Carruthers, E.; Diédhiou, C.; Ahmadou, B.; Soropogui, B.; Ruedas, J.; Peters, K.; Bartkowiak, M.; Mboup, S.; Ben Amor, Y.; Connor, J. H.; Weidemaier, K.; et al. A point-of-care diagnostic for differentiating Ebola from endemic febrile diseases. *Science Translational Medicine. Sci. Transl. Med.* **2018**, *10*, No. eaat0944.

(51) Song, C.; Zhang, J.; Liu, Y.; Guo, X.; Guo, Y.; Jiang, X.; Wang, L. Highly sensitive SERS assay of DENV gene via a cascade signal amplification strategy of localized catalytic hairpin assembly and hybridization chain reaction. *Sens Actuators B Chem.* **2020**, *325*, No. 128970.

(52) Ngo, H. T.; Wang, H. N.; Fales, A. M.; Nicholson, B. P.; Woods, C. W.; Vo-Dinh, T. DNA bioassay-on-chip using SERS detection for dengue diagnosis. *Analyst* **2014**, *139* (22), 5655–5659.

(53) Saleem, M.; Bilal, M.; Anwar, S.; Rehman, A.; Ahmed, M. Optical diagnosis of dengue virus infection in human blood serum using Raman spectroscopy. *Laser Physics Letters* **2013**, *10* (3), 035602.

(54) Khan, S.; Ullah, R.; Saleem, M.; Bilal, M.; Rashid, R.; Khan, I.; Mahmood, A.; Nawaz, M. Raman spectroscopic analysis of dengue virus infection in human blood sera. *Optik* **2016**, *127* (4), 2086–2088.

(55) Khan, S.; Ullah, R.; Khan, A.; Wahab, N.; Bilal, M.; Ahmed, M. Analysis of dengue infection based on Raman spectroscopy and support vector machine (SVM). *Biomed Opt Express* **2016**, *7* (6), 2249–2256.

(56) Khan, S.; Ullah, R.; Khan, A.; Sohail, A.; Wahab, N.; Bilal, M.; Ahmed, M. Random Forest-Based Evaluation of Raman Spectroscopy for Dengue Fever Analysis. *Appl. Spectrosc.* **2017**, *71* (9), 2111–2117.

(57) Mahmood, T.; Nawaz, H.; Ditta, A.; Majeed, M. I.; Hanif, M. A.; Rashid, N.; Bhatti, H. N.; Nargis, H. F.; Saleem, M.; Bonnier, F.; Byrne, H. Raman spectral analysis for rapid screening of dengue infection. *Spectrochim Acta A Mol. Biomol. Spectrosc.* **2018**, *200*, 136–142.

(58) Naseer, K.; Amin, A.; Saleem, M.; Qazi, J. Raman spectroscopy based differentiation of typhoid and dengue fever in infected human sera. *Spectrochim Acta A Mol. Biomol. Spectrosc.* **2019**, *206*, 197–201.

(59) Bilal, M.; Bilal, M.; Saleem, M.; Khurram, M.; Khan, S.; Ullah, R.; Ali, H.; Ahmed, M.; Shahzada, S.; Khan, E. U. Raman spectroscopy based investigation of molecular changes associated with an early stage of dengue virus infection. *Laser Physics* **2017**, *27* (4), 045601.

(60) Othman, N. H. L.; Khuan, Y.; Radzol, A. R. M.; Mansor, W.; Hisham, N. I. A. PCA-QDA Model Selection for Detecting NS1 Related Diseases from SERS Spectra of Salivary Mixtures. In *World Congress on Medical Physics and Biomedical Engineering*; Lhotska, L.; Sukupova, L.; Lacković, I.; Ibbott, G. S., Eds.; Springer, 2019.

(61) Radzol, A. R. M. L.; K Y; Mansor, W.; Ariffin, N. Biostatistical analysis of principal component of salivary Raman spectra for NS1 infection. *IEEE EMBS Conference on Biomedical Engineering and Sciences* **2016**, 13–18.

(62) Desai, S.; Mishra, S. V.; Joshi, A.; Sarkar, D.; Hole, A.; Mishra, R.; Dutt, S.; Chilakapati, M. K.; Gupta, S.; Dutt, A. Raman spectroscopy-based detection of RNA viruses in saliva: A preliminary report. *J. Biophotonics* **2020**, *13* (10), No. e202000189.

(63) Sánchez-Purrà, M.; Carre-Camps, M.; de Puig, H.; Bosch, I.; Gehrke, L.; Hamad-Schifferli, K. Surface-Enhanced Raman Spectroscopy-Based Sandwich Immunoassays for Multiplexed Detection of Zika and Dengue Viral Biomarkers. *ACS Infect. Dis.* **2017**, *3* (10), 767–776.

(64) Camacho, S. A.; Sobral-Filho, R. G.; Aoki, P. H. B.; Constantino, C. J. L.; Brolo, A. G. Zika Immunoassay Based on Surface-Enhanced Raman Scattering Nanoprobes. *ACS Sens* **2018**, *3* (3), 587–594.

(65) Tripathi, M. N.; Jangir, P.; Aakriti; Rai, S.; Gangwar, M.; Nath, G.; Saxena, P. S.; Srivastava, A. A novel approach for rapid and sensitive detection of Zika virus utilizing silver nanoislands as SERS platform. *Spectrochim Acta A Mol. Biomol. Spectrosc.* **2023**, *302*, No. 123045.

(66) Silge, A.; Bocklitz, T.; Becker, B.; Matheis, W.; Popp, J.; Bekerjian-Ding, I. Raman spectroscopy-based identification of toxoid vaccine products. *NPJ Vaccines* **2018**, *3*, 50.

(67) *Global Poliovirus Containment Action Plan 2022–2024*; World Health Organization, 2022.

(68) Alexander, T. A. Development of methodology based on commercialized SERS-active substrates for rapid discrimination of Poxviridae virions. *Anal. Chem.* **2008**, *80* (8), 2817–2825.

(69) Alexander, T. A. Surface-enhanced Raman spectroscopy: A new approach to rapid identification of intact viruses. *Spectroscopy* **2008**, *23* (7), 36.

(70) Zhang, Z.; Jiang, H.; Jiang, S.; Dong, T.; Wang, X.; Wang, Y.; Li, Y. Rapid Detection of the Monkeypox Virus Genome and Antigen Proteins Based on Surface-Enhanced Raman Spectroscopy. *ACS Appl. Mater. Interfaces* **2023**, *15* (29), 34419–34426.

(71) Yu, Q.; Li, J.; Zheng, S.; Xia, X.; Xu, C.; Wang, C.; Wang, C.; Gu, B. Molybdenum disulfide-loaded multilayer AuNPs with colorimetric-SERS dual-signal enhancement activities for flexible immunochromatographic diagnosis of monkeypox virus. *J. Hazard Mater.* **2023**, *459*, No. 132136.

(72) Lv, X.; Zhang, Z.; Zhao, Y.; Sun, X.; Jiang, H.; Zhang, S.; Sun, X.; Qiu, X.; Li, Y. Label-free detection of virus based on surface-enhanced Raman scattering. *Spectrochim Acta A Mol. Biomol. Spectrosc.* **2023**, *302*, No. 123087.

(73) Cornish, N. E.; Anderson, N. L.; Arambula, D. G.; Arduino, M. J.; Bryan, A.; Burton, N. C.; Chen, B.; Dickson, B. A.; Giri, J. G.; Griffith, N. K.; et al. Clinical Laboratory Biosafety Gaps: Lessons Learned from Past Outbreaks Reveal a Path to a Safer Future. *Clin Microbiol Rev.* **2021**, *34* (3), No. e0012618.

(74) Mazzola, L. T.; Kelly-Cirino, C. Diagnostics for Lassa fever virus: a genetically diverse pathogen found in low-resource settings. *BMJ Glob Health* **2019**, *4* (Suppl2), No. e001116.

(75) Filip, R.; Gheorghita Puscaselu, R.; Anchin-Norocel, L.; Dimian, M.; Savage, W. K. Global Challenges to Public Health Care Systems during the COVID-19 Pandemic: A Review of Pandemic Measures and Problems. *J. Pers Med.* **2022**, *12* (8), 1295.

(76) Goulart, A. C. C.; Silveira, L., Jr.; Carvalho, H. C.; Dorta, C. B.; Pacheco, M. T. T.; Zangaro, R. A. Diagnosing COVID-19 in human serum using Raman spectroscopy. *Lasers Med. Sci.* **2022**, *37* (4), 2217–2226.

(77) Awada, C.; Abdullah, M. M. B.; Traboulsi, H.; Dab, C.; Alshoaibi, A. SARS-CoV-2 Receptor Binding Domain as a Stable-Potential Target for SARS-CoV-2 Detection by Surface-Enhanced Raman Spectroscopy. *Sensors* **2021**, *21* (13), 4617.

- (78) Yin, G.; Li, L.; Lu, S.; Yin, Y.; Su, Y.; Zeng, Y.; Luo, M.; Ma, M.; Zhou, H.; Orlandini, L.; et al. An efficient primary screening of COVID-19 by serum Raman spectroscopy. *J. Raman Spectrosc.* **2021**, *52* (5), 949–958.
- (79) Carlomagno, C.; Bertazioli, D.; Gualerzi, A.; Picciolini, S.; Banfi, P. I.; Lax, A.; Messina, E.; Navarro, J.; Bianchi, L.; Caronni, A.; et al. COVID-19 salivary Raman fingerprint: innovative approach for the detection of current and past SARS-CoV-2 infections. *Sci. Rep.* **2021**, *11* (1), No. 4943.
- (80) Ember, K.; Daoust, F.; Mahfoud, M.; Dallaire, F.; Ahmad, E. Z.; Tran, T.; Plante, A.; Diop, M. K.; Nguyen, T.; St-Georges-Robillard, A.; et al. Saliva-based detection of COVID-19 infection in a real-world setting using reagent-free Raman spectroscopy and machine learning. *J. Biomed. Opt.* **2022**, *27* (2), 025002 DOI: 10.1117/1.JBO.27.2.025002.
- (81) Farhane, Z.; Bonnier, F.; Casey, A.; Maguire, A.; O'Neill, L.; Byrne, H. J. Cellular discrimination using in vitro Raman micro spectroscopy: the role of the nucleolus. *Analyst* **2015**, *140* (17), 5908–5919.
- (82) Goulart, A. C. C.; Zangaro, R. A.; Carvalho, H. C.; Lednev, I. K.; Silveira, L., Jr. Diagnosing COVID-19 in nasopharyngeal secretion through Raman spectroscopy: a feasibility study. *Lasers Med. Sci.* **2023**, *38* (1), 210.
- (83) Goulart, A. C. C.; Zangaro, R. A.; Carvalho, H. C.; Silveira, L., Jr. Diagnosing COVID-19 in human sera with detected immunoglobulins IgM and IgG by means of Raman spectroscopy. *J. Raman Spectrosc.* **2021**, *52* (12), 2671–2682.
- (84) Guan, P. C.; Zhang, H.; Li, Z. Y.; Xu, S. S.; Sun, M.; Tian, X. M.; Ma, Z.; Lin, J. S.; Gu, M. M.; Wen, H.; et al. Rapid Point-of-Care Assay by SERS Detection of SARS-CoV-2 Virus and Its Variants. *Anal. Chem.* **2022**, *94* (51), 17795–17802.
- (85) Pezzotti, G.; Boschetto, F.; Ohgiani, E.; Fujita, Y.; Shin-Ya, M.; Adachi, T.; Yamamoto, T.; Kanamura, N.; Marin, E.; Zhu, W.; et al. Raman Molecular Fingerprints of SARS-CoV-2 British Variant and the Concept of Raman Barcode. *Adv. Sci.* **2022**, *9* (3), No. e2103287.
- (86) Rumaling, M. I.; Chee, F. P.; Bade, A.; Goh, L. P. W.; Juhim, F. Biofingerprint detection of corona virus using Raman spectroscopy: a novel approach. *SN Appl. Sci.* **2023**, *5* (7), 197 DOI: 10.1007/s42452-023-05419-3.
- (87) Huang, J.; Wen, J.; Zhou, M.; Ni, S.; Le, W.; Chen, G.; Wei, L.; Zeng, Y.; Qi, D.; Pan, M.; et al. On-Site Detection of SARS-CoV-2 Antigen by Deep Learning-Based Surface-Enhanced Raman Spectroscopy and Its Biochemical Foundations. *Anal. Chem.* **2021**, *93* (26), 9174–9182.
- (88) Yang, Y.; Peng, Y.; Lin, C.; Long, L.; Hu, J.; He, J.; Zeng, H.; Huang, Z.; Li, Z. Y.; Tanemura, M.; et al. Human ACE2-Functionalized Gold Virus-Trap Nanostructures for Accurate Capture of SARS-CoV-2 and Single-Virus SERS Detection. *Nanomicro Lett.* **2021**, *13*, 109.
- (89) Yeh, Y. J.; Le, T. N.; Hsiao, W. W.; Tung, K. L.; Ostrikov, K. K.; Chiang, W. H. Plasmonic nanostructure-enhanced Raman scattering for detection of SARS-CoV-2 nucleocapsid protein and spike protein variants. *Anal. Chim. Acta* **2023**, *1239*, No. 340651.
- (90) Garsuault, D.; El Messaoudi, S.; Prabakaran, M.; Cheong, I.; Boulanger, A.; Schmitt-Boulanger, M. Detection of several respiratory viruses with Surface-Enhanced Raman Spectroscopy coupled with Artificial Intelligence. *Clinical Spectroscopy* **2023**, *5*, 100025.
- (91) Khlebtsov, B.; Khlebtsov, N. Surface-Enhanced Raman Scattering-Based Lateral-Flow Immunoassay. *Nanomaterials* **2020**, *10* (11), 2228.
- (92) Chen, H.; Park, S. G.; Choi, N.; Kwon, H. J.; Kang, T.; Lee, M. K.; Choo, J. Sensitive Detection of SARS-CoV-2 Using a SERS-Based Aptasensor. *ACS Sens* **2021**, *6* (6), 2378–2385.
- (93) Yang, Y.; Zhao, R.; Wang, Y.; Song, D.; Jiang, B.; Guo, X.; Liu, W.; Long, F.; Song, H.; Hao, R. Rapid and universal detection of SARS-CoV-2 and influenza A virus using a reusable dual-channel optic fiber immunosensor. *J. Med. Virol.* **2022**, *94* (11), 5325–5335.
- (94) Chen, J.; Yu, Q.; Lu, M.; Jeon, C. S.; Pyun, S. H.; Choo, J. A strategy to enhance SERS detection sensitivity through the use of SiO<sub>2</sub> beads in a 1536-well plate. *Anal Bioanal Chem.* **2023**, *415* (24), 5939–5948.
- (95) Mousavi, S. M.; Hashemi, S. A.; Rahmiani, V.; Kalashgrani, M. Y.; Gholami, A.; Omidifar, N.; Chiang, W. H. Highly Sensitive Flexible SERS-Based Sensing Platform for Detection of COVID-19. *Biosensors* **2022**, *12* (7), 466.
- (96) Ebbah, E.; Amisshah, A.; Kim, J. H.; Driskell, J. D. SERS-based immunoassay on a plasmonic syringe filter for improved sampling and labeling efficiency of biomarkers. *Analyst* **2023**, *149* (1), 221–230.
- (97) Salehi, H.; Ramoji, A.; Mougari, S.; Merida, P.; Neyret, A.; Popp, J.; Horvat, B.; Muriaux, D.; Cuisinier, F. Specific intracellular signature of SARS-CoV-2 infection using confocal Raman microscopy. *Commun. Chem.* **2022**, *5* (1), 85.
- (98) Peng, Y.; Lin, C.; Long, L.; Masaki, T.; Tang, M.; Yang, L.; Liu, J.; Huang, Z.; Li, Z.; Luo, X.; et al. Charge-Transfer Resonance and Electromagnetic Enhancement Synergistically Enabling MXenes with Excellent SERS Sensitivity for SARS-CoV-2 S Protein Detection. *Nanomicro Lett.* **2021**, *13*, 52.
- (99) Sanchez, J. E.; Jaramillo, S. A.; Settles, E.; Velazquez Salazar, J. J.; Lehr, A.; Gonzalez, J.; Rodriguez Aranda, C.; Navarro-Contreras, H. R.; Raniere, M. O.; Harvey, M.; et al. Detection of SARS-CoV-2 and its S and N proteins using surface enhanced Raman spectroscopy. *RSC Adv.* **2021**, *11* (41), 25788–25794.
- (100) Song, K.; Xue, W.; Li, X.; Chang, Y.; Liu, M. Self-Assembly of Single-Virus SERS Hotspots for Highly Sensitive In Situ Detection of SARS-CoV-2 on Solid Surfaces. *Anal. Chem.* **2024**, *96* (21), 8830–8836.
- (101) Jadhav, S. A.; Biji, P.; Panthalingal, M. K.; Murali Krishna, C.; Rajkumar, S.; Joshi, D. S.; Sundaram, N. Development of integrated microfluidic platform coupled with Surface-enhanced Raman Spectroscopy for diagnosis of COVID-19. *Med. Hypotheses* **2021**, *146*, No. 110356.
- (102) Sitjar, J.; Xu, H. Z.; Liu, C. Y.; Wang, J. R.; Liao, J. D.; Tsai, H. P.; Lee, H.; Liu, B. H.; Chang, C. W. Synergistic surface-enhanced Raman scattering effect to distinguish live SARS-CoV-2 S pseudovirus. *Anal. Chim. Acta* **2022**, *1193*, No. 339406.
- (103) Sitjar, J.; Liao, J. D.; Lee, H.; Tsai, H. P.; Wang, J. R.; Chen, C. H.; Wang, H.; Liu, B. H. Detection of live SARS-CoV-2 virus and its variants by specially designed SERS-active substrates and spectroscopic analyses. *Anal. Chim. Acta* **2023**, *1256*, No. 341151.
- (104) Zhou, L.; Vestri, A.; Marchesano, V.; Rippa, M.; Sagnelli, D.; Picazio, G.; Fusco, G.; Han, J.; Zhou, J.; Petti, L. The Label-Free Detection and Identification of SARS-CoV-2 Using Surface-Enhanced Raman Spectroscopy and Principal Component Analysis. *Biosensors* **2023**, *13* (12), 1014.
- (105) Akdeniz, M.; Al-Shaebi, Z.; Altunbek, M.; Bayraktar, C.; Kayabolen, A.; Bagci-Onder, T.; Aydin, O. Characterization and discrimination of spike protein in SARS-CoV-2 virus-like particles via surface-enhanced Raman spectroscopy. *Biotechnol. J.* **2024**, *19* (1), No. e2300191.
- (106) Robertson, J. L.; Senger, R. S.; Talty, J.; Du, P.; Sayed-Issa, A.; Avellar, M. L.; Ngo, L. T.; Gomez De La Espriella, M.; Fazili, T. N.; Jackson-Akers, J. Y.; et al. Alterations in the molecular composition of COVID-19 patient urine, detected using Raman spectroscopic/computational analysis. *PLoS One* **2022**, *17* (7), No. e0270914.
- (107) Pahlow, S.; Richard-Lacroix, M.; Hornung, F.; Kose-Vogel, N.; Mayerhofer, T. G.; Hniopek, J.; Ryabchykov, O.; Bocklitz, T.; Weber, K.; Ehrlich, R.; et al. Simple, Fast and Convenient Magnetic Bead-Based Sample Preparation for Detecting Viruses via Raman-Spectroscopy. *Biosensors* **2023**, *13* (6), 594.
- (108) Zhang, D.; Zhang, X.; Ma, R.; Deng, S.; Wang, X.; Wang, X.; Zhang, X.; Huang, X.; Liu, Y.; Li, G.; et al. Ultra-fast and onsite interrogation of Severe Acute Respiratory Syndrome Coronavirus 2 (SARS-CoV-2) in waters via surface enhanced Raman scattering (SERS). *Water Res.* **2021**, *200*, No. 117243.
- (109) Kim, K.; Kashefi-Kheyraadi, L.; Joung, Y.; Kim, K.; Dang, H.; Chavan, S. G.; Lee, M. H.; Choo, J. Recent advances in sensitive surface-enhanced Raman scattering-based lateral flow assay platforms for point-of-care diagnostics of infectious diseases. *Sens Actuators B Chem.* **2021**, *329*, No. 129214.

- (110) Mo, W.; Wen, J.; Huang, J.; Yang, Y.; Zhou, M.; Ni, S.; Le, W.; Wei, L.; Qi, D.; Wang, S.; et al. Classification of Coronavirus Spike Proteins by Deep-Learning-Based Raman Spectroscopy and its Interpretative Analysis. *J. Appl. Spectrosc.* **2023**, *89* (6), 1203–1211.
- (111) Lu, X.; Liu, Q.; Benavides-Montano, J. A.; Nicola, A. V.; Aston, D. E.; Rasco, B. A.; Aguilar, H. C. Detection of receptor-induced glycoprotein conformational changes on enveloped virions by using confocal micro-Raman spectroscopy. *J. Virol* **2013**, *87* (6), 3130–3142.
- (112) Neng, J.; Li, Y.; Driscoll, A. J.; Wilson, W. C.; Johnson, P. A. Detection of Multiple Pathogens in Serum Using Silica-Encapsulated Nanotags in a Surface-Enhanced Raman Scattering-Based Immunoassay. *J. Agric. Food Chem.* **2018**, *66* (22), 5707–5712.
- (113) Zhang, H.; Harpster, M. H.; Wilson, W. C.; Johnson, P. A. Surface-enhanced Raman scattering detection of DNAs derived from virus genomes using Au-coated paramagnetic nanoparticles. *Langmuir* **2012**, *28* (8), 4030–4037.
- (114) Neng, J.; Harpster, M. H.; Wilson, W. C.; Johnson, P. A. Surface-enhanced Raman scattering (SERS) detection of multiple viral antigens using magnetic capture of SERS-active nanoparticles. *Biosens. Bioelectron.* **2013**, *41*, 316–321.
- (115) Zong, C.; Xu, M.; Xu, L. J.; Wei, T.; Ma, X.; Zheng, X. S.; Hu, R.; Ren, B. Surface-Enhanced Raman Spectroscopy for Bioanalysis: Reliability and Challenges. *Chem. Rev.* **2018**, *118* (10), 4946–4980.
- (116) Kharbach, M.; Alaoui Mansouri, M.; Taabouz, M.; Yu, H. Current Application of Advancing Spectroscopy Techniques in Food Analysis: Data Handling with Chemometric Approaches. *Foods* **2023**, *12* (14), 2753.
- (117) Marzi, J.; Fuhrmann, E.; Brauchle, E.; Singer, V.; Pfannstiel, J.; Schmidt, I.; Hartmann, H. Non-Invasive Three-Dimensional Cell Analysis in Bioinks by Raman Imaging. *ACS Appl. Mater. Interfaces* **2022**, *14* (27), 30455–30465.
- (118) Eberhardt, K. S.; Matthäus, C.; Schmitt, C.; Popp, M. J. Advantages and limitations of Raman spectroscopy for molecular diagnostics: An update. *Expert Rev. Mol. Diagn.* **2015**, *15* (6), 773–787.
- (119) Storozhuk, D.; Ryabchykov, O.; Popp, J.; Bocklitz, T. *RAMANMETRIX: A Delightful Way to Analyze Raman Spectra*, 2022, arXiv:2201.07586. arXiv.org e-Print archive <https://arxiv.org/abs/2201.07586>.
- (120) Ramanmetrix. *RAMANMETRIX Software Documentation*, 2021.
- (121) Zu, Y.; Chang, H.; Cui, Z. Molecular point-of-care testing technologies: Current status and challenges. *Nexus* **2025**, *2* (2), No. 100059.
- (122) Food, U. S.; Drug, A. Overview of Device Regulation *Device Advice: Comprehensive Regulatory Assistance*, 2025.
- (123) Regulation (EU) 2017/746 of the European Parliament and of the Council of 5 April 2017 on *in vitro* diagnostic medical devices and repealing Directive 98/79/EC and Commission Decision 2010/227/EU. 2010, Vol. L 117 176 332.
- (124) Food, U. S.; Drug, A. Artificial Intelligence in Software as a Medical Device. *Software as a Medical Device (SaMD)—Device Advice: Comprehensive Regulatory Assistance*. 2025, (accessed 2025/08/21).
- (125) Bottini, M.; Ryu, S. J.; Terander, A. E.; Voglis, S.; Maldaner, N.; Bellut, D.; Regli, L.; Serra, C.; Staartjes, V. E. The Ever-Evolving Regulatory Landscape Concerning Development and Clinical Application of Machine Intelligence: Practical Consequences for Spine Artificial Intelligence Research. *Neurospine* **2025**, *22* (1), 134–143.
- (126) Artika, I. M.; Ma'roef, C. N. Laboratory biosafety for handling emerging viruses. *Asian Pac. J. Trop. Biomed.* **2017**, *7* (5), 483–491.
- (127) Dolzkiy, A. A.; Grishchenko, I. V.; Yudkin, D. V. Cell Cultures for Virology: Usability, Advantages, and Prospects. *Int. J. Mol. Sci.* **2020**, *21* (21), 7978.
- (128) Selo, M. A.; Sake, J. A.; Kim, K. J.; Ehrhardt, C. In vitro and ex vivo models in inhalation biopharmaceutical research - advances, challenges and future perspectives. *Adv. Drug Delivery Rev.* **2021**, *177*, No. 113862.
- (129) Colby, L. A.; Quenee, L. E.; Zitzow, L. A. Considerations for infectious disease research studies using animals. In *Comparative Medicine* 2017; Vol. 67, pp 222–231.
- (130) Klingstrom, T.; Bongcam-Rudloff, E.; Reichel, J. Legal & ethical compliance when sharing biospecimen. *Brief Funct. Genomics* **2018**, *17* (1), 1–7.
- (131) Srivastava, S.; Sharma, D.; Kumar, S.; Sharma, A.; Rijal, R.; Asija, A.; Adhikari, S.; Rustagi, S.; Sah, S.; Al-Qaim, Z. H.; et al. Emergence of Marburg virus: a global perspective on fatal outbreaks and clinical challenges. *Front. Microbiol.* **2023**, *14*, No. 1239079.
- (132) Vitti, J. N.; Vitti, R.; Chu, K.; Mellis, S. The ethics of clinical research in the era of COVID-19. *Front Public Health* **2024**, *12*, No. 1359654.
- (133) Selgelid, M. J. Gain-of-Function Research: Ethical Analysis. *Sci. Eng. Ethics* **2016**, *22* (4), 923–964.
- (134) Belsler, J. A.; Kieran, T. J.; Mitchell, Z. A.; Sun, X.; Mayfield, K.; Tumpey, T. M.; Spengler, J. R.; Maines, T. R. Key considerations to improve the normalization, interpretation and reproducibility of morbidity data in mammalian models of viral disease. *Dis. Model Mech.* **2024**, *17* (3), dmm050511 DOI: 10.1242/dmm.050511.
- (135) Masopust, D.; Sivula, C. P.; Jameson, S. C. Of Mice, Dirty Mice, and Men: Using Mice To Understand Human Immunology. *J. Immunol.* **2017**, *199* (2), 383–388.
- (136) Zabidi, N. Z.; Liew, H. L.; Farouk, I. A.; Puniyamurti, A.; Yip, A. J. W.; Wijesinghe, V. N.; Low, Z. Y.; Tang, J. W.; Chow, V. T. K.; Lal, S. K. Evolution of SARS-CoV-2 Variants: Implications on Immune Escape, Vaccination, Therapeutic and Diagnostic Strategies. *Viruses* **2023**, *15* (4), 944.
- (137) Hartman, K. A.; Clayton, N.; Thomas, G. J., Jr. Studies of Virus Structure by Raman Spectroscopy. I. R17 Virus and R17 RNA. *Biochem. Biophys. Res. Commun.* **1973**, *50* (3), 942–949.
- (138) Thomas, G. J., Jr.; Prescott, B.; McDonald-Ordzie, P. E.; Hartman, K. A. Studies of Virus Structure by Laser Raman Spectroscopy. II. MS2 Phage, MS2 Capsids, and MS2 RNA in Aqueous Solutions. *J. Mol. Biol.* **1976**, *102* (1), 103–124.
- (139) Thomas, G. J.; Prescott, B.; Day, L. A. Structure Similarity, Difference, and Variability in the Filamentous Viruses fd, If1, IKE, Pf1, and Xf Investigated by Laser Raman Spectroscopy. *J. Mol. Biol.* **1983**, *165* (2), 321–356.
- (140) Wen, Z.-Q.; Thomas, G. J., Jr. UV Resonance Raman Spectroscopy of DNA and Protein Constituents of Viruses: Assignments and Cross Sections for Excitations at 257, 244, 238, and 229 nm. *Biopolymers* **1998**, *45* (3), 247–256.
- (141) Moor, K.; Terada, Y.; Taketani, A.; Matsuyoshi, H.; Ohtani, K.; Sato, H. Early Detection of Virus Infection in Live Human Cells Using Raman Spectroscopy. *J. Biomed. Opt.* **2018**, *23* (9), No. 097001.
- (142) El-Mashtoly, S. F.; Gerwert, K. Diagnostics and Therapy Assessment Using Label-Free Raman Imaging. *Anal. Chem.* **2022**, *94* (1), 120–142.
- (143) Marotta, N. E. Patterned Nanoarray SERS Substrates for Pathogen Detection. Ph.D. Thesis. Georgia Institute of Technology: Atlanta, GA, 2010.
- (144) Sigle, M.; Rohlfing, K.; Kenny, M.; Scheuermann, S.; Sun, N.; Graebner, U.; Haug, V.; Sudmann, J.; Seitz, C. M.; Heinzmann, D.; Schenke-Layland, K.; Maguire, P. B.; Walch, A.; Marzi, J.; Gawaz, M. P. Translating Genomic Tools to Raman Spectroscopy Analysis Enables High-Dimensional Tissue Characterization at Molecular Resolution. *Nat. Commun.* **2023**, *14*, No. 5799.
- (145) Gahlaut, S. K.; Savargaonkar, D.; Sharan, C.; Yadav, S.; Mishra, P.; Singh, J. P. SERS Platform for Dengue Diagnosis from Clinical Samples Employing a Hand Held Raman Spectrometer. *Anal. Chem.* **2020**, *92* (3), 2527–2534.
- (146) Gordon, J.; Mousavi, S. D.; Li, J.; Filippone, N.; Walter, L.; Cheng, H.-W.; Skeete, Z.; Feldman, H.; Hakimi, S.; Cappuccio, K.; Wang, S.; Hader, M.; Shang, G.; Turner, J.; Cameron, A.; Bane, S.; Poliks, M.; Lu, S.; Yuan, T. T.; Zhong, C.-J. Plasmonic Nanoprobe-Enabled SERS Detection of SARS-CoV-2 Proteins and Virus Samples on Wax-Printed Paper Substrates. *Anal. Chem.* **2025**, *97* (46), 21303–21313.
- (147) Plavec, Z.; Domanska, A.; Liu, X.; Laine, P.; Paulin, L.; Varjosalo, M.; Auvinen, P.; Wolf, S. G.; Anastasina, M.; Butcher, S. J.

SARS-CoV-2 Production, Purification Methods and UV Inactivation for Proteomics and Structural Studies. *Viruses* **2022**, *14* (9), 1989.

(148) Pestov, D.; Murawski, R. K.; Ariunbold, G. O.; Wang, X.; Zhi, M.; Sokolov, A. V.; Sautenkov, V. A.; Rostovtsev, Y. V.; Dogariu, A.; Huang, Y.; Scully, M. O. Optimizing the laser-pulse configuration for coherent Raman spectroscopy. *Science*. **2007**, *316* (5822), 265–268.

(149) Wang, Y.; Ruan, Q.; Lei, Z. C.; Lin, S. C.; Zhu, Z.; Zhou, L.; Yang, C. Highly Sensitive and Automated Surface Enhanced Raman Scattering-based Immunoassay for H5N1 Detection with Digital Microfluidics. *Anal. Chem.* **2018**, *90*, 5224–5231.

(150) Chang, Y.; Wang, Y.; Li, W.; Wei, Z.; Tang, S.; Chen, R. Mechanisms, Techniques and Devices of Airborne Virus Detection: A Review. *Int. J. Environ. Res. Public Health* **2023**, *20*, 5471.